Design Optimization of Active Trailer Differential Braking Systems for Car-Trailer Combinations

By

Eungkil Lee

A thesis

presented in fulfillment of

the requirement for the degree of

Master of Applied Science

in

Automotive Engineering

Faculty of Engineering and Applied Science

University of Ontario Institute of Technology

Oshawa, Ontario, Canada, 2016

Dedicated to

My family in Korea

and my wife Jihye Kim

Thanks for their support, encouragement and love.

Abstract

The thesis studies active trailer differential braking (ATDB) systems to improve the lateral stability of car-trailer (CT) combinations. CT combinations exhibit unique unstable motion modes, including jack-knifing, trailer sway, and roll-over. To address this CT stability problem, two ATDB controllers are proposed, which are designed using the Linear Quadratic Regulator (LQR) and H_∞ robust control techniques. In order to design the ATDB controllers, a linear 3 degrees of freedom (DOF) and a linear 5-DOF model are generated and validated with a nonlinear CT model derived using CarSim software. Eigenvalue analysis is conducted to examine the effects of typical trailer parameters on the lateral stability of CT combinations. The contribution of the LQR-based ATDB controller to the enhancement of CT stability is assessed. The thesis also investigates the insensitivity of the H_∞ controller to parameter uncertainties. A genetic algorithm (GA) is applied to find optimal control variables of the active safety systems. Numerical simulations demonstrate that the parametric study may provide a guideline for trailer design variable selections, and the proposed ATDB systems can effectively increase the safety of CT combinations.

Acknowledgement

I would like to express my deep gratitude to my master thesis supervisor, Dr. Yuping He, for his support, encouragement and guidance during this research. Without him, this work would not have been possible. I would also like to thank my family and all my friends at UOIT for their help and encouraging me over the past two years. Last but not the least important, thank you to my wife, Jihye Kim, who has been patient with and supportive of this journey.

Table of Contents

List of Figures

List of Tables

Nomenclature

a	Longitudinal distance between the center of gravity of the car and front axle of the car
b	Longitudinal distance between the center of gravity of the car and rear axle of the car
d	Longitudinal distance between the center of gravity of the car and hitch
e	Longitudinal distance between the center of gravity of the trailer and hitch
f	Longitudinal distance between the center of gravity of the trailer and axle of the trailer
h_1	Height of the center of gravity of car sprung mass above roll axis
h_2	Height of the center of gravity of trailer sprung mass above roll axis
z_1	Vertical distance between car roll center and hitch
z_2	Vertical distance between trailer roll center and hitch
cr_1	Roll damping coefficient of the car suspension
cr_2	Roll damping coefficient of the trailer suspension
kr_1	Roll stiffness of the car suspension
kr_2	Roll stiffness of the trailer suspension
m_c	Car total mass

m_{cs}	Car sprung mass
m_t	Trailer total mass
m_{ts}	Trailer sprung mass
I_{z1}	Yaw moment of inertia of the total mass of the car
I_{z2}	Yaw moment of inertia of the total mass of the trailer
I_{xx1}	Roll moment of inertia of the sprung mass of the car
I_{xx2}	Roll moment of inertia of the sprung mass of the trailer
I_{xz1}	Roll-yaw product of inertial of the sprung mass of the car
I_{xz2}	Roll- yaw product of inertial of the sprung mass of the trailer
C_1	Cornering stiffness of the front tire of the car
C_2	Cornering stiffness of the rear tire of the car
C_3	Cornering stiffness of the tire of the trailer
α_1	Side-slip angle of the front tire of the car
α_2	Side-slip angle of the rear tire of the car
α_3	Side-slip angle of the tire of the trailer
δ	Car front wheel steering angle
U_c	The forward speed of the car
U_t	The forward speed of the trailer
V_c	Lateral velocity of the car

V_t	Lateral velocity of the trailer
r_c	Yaw rate of the car
r_t	Yaw rate of the trailer
ϕ_c	Roll angle of the sprung mass of the car
ϕ_t	Roll angle of the sprung mass of the trailer
F_{y1}	Lateral force of the front tire of the car
F_{y2}	Lateral force of the rear tire of the car
F_{y3}	Lateral force of the tire of the trailer
F_{yt}	Lateral force at the hitch
F_{x1}	Longitudinal force of the front tire of the car
F_{x2}	Longitudinal force of the rear tire of the car
F_{x3}	Longitudinal force of the tire of the trailer
F_{xt}	Longitudinal force at the hitch
ψ	Articulation angle between car and trailer
M_z	Active yaw moment
ADAMS	Automated dynamic analysis and design system
AFS	Active four wheel steering
AHV	Articulated heavy vehicle
ARS	Active rear wheel steering

ASS	Active safety system
ATDB	Active trailer differential braking
ATS	Active trailer steering
CG	Center of gravity
CT	Car-trailer
DADS	Dynamic analysis and design system
DHIL	Driver-hardware-in-the-loop
DOF	Degrees of freedom
DSIL	Drive-software-in-the-loop
DTAHV	Double-trailer articulated heavy vehicle
DYM	Direct yaw moment
ESC	Electronic stability control
GA	Genetic algorithm
LQR	Linear quadratic regulator
PFOT	Path-following-off-tracking
PID	Proportional-integral-derivative
RMS	Root mean square
RWA	Rearward amplification
VGA	Variable geometry approach

1.Introduction

1.1 Car-Trailer Combinations

The vehicles mainly researched in this thesis are car-trailer (CT) combinations. Generally, a CT combination consists of a towing unit, such as a pick-up truck or passenger car, and a towed unit, namely a trailer, and the leading and trailing vehicle units are connected at an articulation point by a hitch [1]. A trailer may be featured with a single axle or double axles. Compared to a single axle trailer, the one with double axles could carry more freight and may be more stable at high-speed maneuver [2]. A single axle trailer is more prone to have stability problem in highway operations. In this thesis, a single axle trailer is considered and researched to improve the lateral stability of CT systems. Figures 1-1 and 1-2 show the typical configuration of a single axle trailer and the one with double axles, respectively.

Figure 1-1. The configuration of a single axle trailer [2]

Figure 1-2. The configuration of a tandem axle trailer [2]

1.2 Motivations

To increase safety of single-unit vehicles (e.g., passenger cars), the United States Government has established FMVSS 126, a vehicle standard that requires all vehicles sold in North America to include an electronic stability control (ESC) system starting in 2012 [53]. An ESC system has the ability to produce a yaw moment for enhancing the lateral stability of the vehicle without driver intervention. Simulations and tests demonstrate that vehicle stability and path-following performance under emergency maneuvers at high lateral accelerations can be improved with ESC systems [54]. However, nearly all the ESC systems are designed for single-unit vehicles and take no account of external loads, e.g., trailers [50].

A trailer is often attached to a passenger car or a pick-up truck in order to tow boats, moving materials and recreational items in North America. Compared to single unit vehicles, CT combinations can carry more freight and reduce fuel consumption [3]. This may be the main reason why CT combinations are widely used in North America. Despite of many benefits, CT combinations may exhibit poor yaw and roll stability because of their multi-unit structures. It has been reported that CT combinations show unique unstable motion modes, including jack-knifing, trailer sway, and roll-over [4-7].

Jack-knifing means the folding of articulated vehicle units, in which the car and trailer form a "V" shape instead of being pulled in a straight line [8]. The Jack-knifing is one of the main causes for fatal accidents of CT combinations [9]. The main problem is losing yaw stability of the CT systems, caused by either braking or combined braking and steering operations coupled with tire force saturation (wheel lock) of the car or trailer [10]. Figure 1-3 shows the jack-knifing of a CT combination.

The second type of unstable motion modes is trailer sway, also known as fish tailing, snaking or tail swing. Trailer sway is a motion mode, in which the towed unit moves side to side behind the towing unit [11]. The trailer sway is usually associated with a high speed and external disturbances (e.g. uneven road, side wind gust and driver steering input) on the trailer unit [12]. There are internal factors as well. Excessive trailer weight, poor trailer weight distribution, high trailer center of gravity (CG),

poor hitch adjustment and low or uneven tire pressure may cause the trailer sway. Figure 1-4 shows the trailer sway of a CT combination.

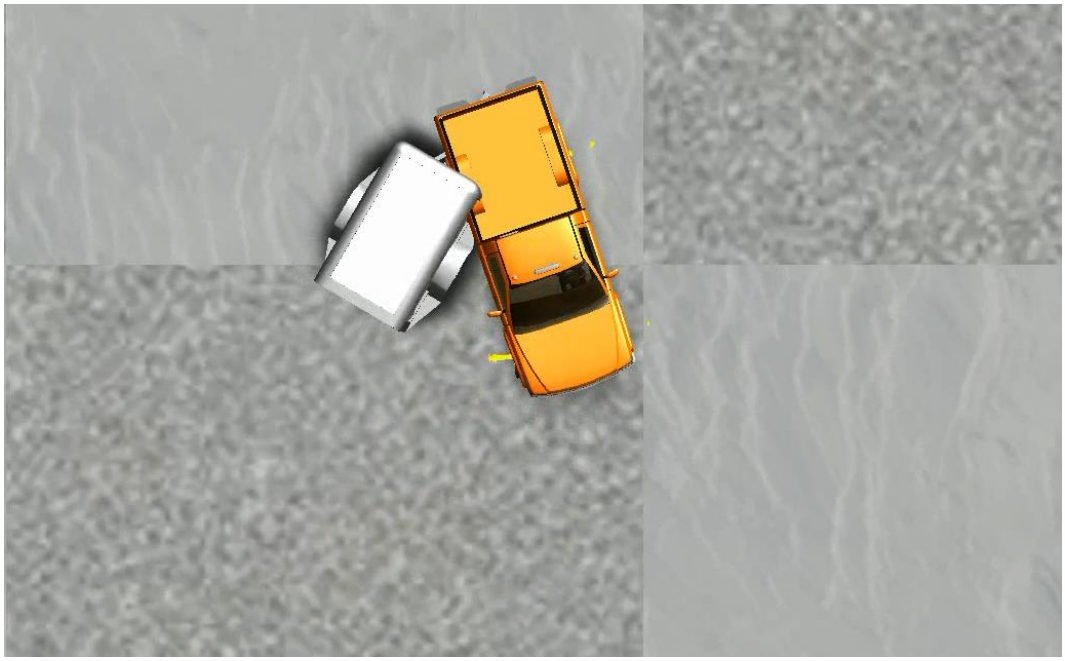

Figure 1-3. The jack-knifing of a CT combinations

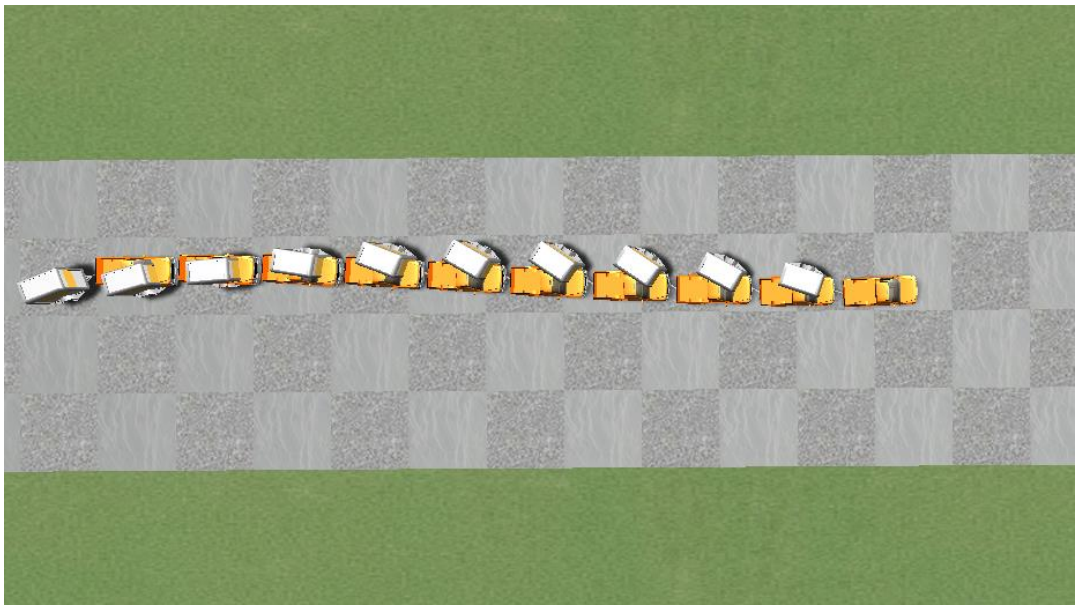

Figure 1-4. The trailer sway of a CT combination

The last type of unstable motion modes is roll-over. Roll-over means that a vehicle turns over onto its side or roof. Roll-over accidents are dangerous, which may lead to a higher fatality rate than other kinds of vehicle crashes [13]. The roll-over usually occurs when high lateral forces are applied on the vehicle under a sharp turning maneuver at high speeds [14]. It means that a roll-over occurs when the lateral acceleration of the vehicle exceeds a roll-over threshold. Figure 1-5 shows the roll-over of a CT combination.

It is important for drivers to be aware of the stability problems while driving CT combinations. However, it is generally difficult for a driver, who doesn't have enough experience and good understanding of a CT combination, to perceive the motion cues of the trailing unit [6, 14]. Even if a driver can recognize the unstable CT motions, he/she may not have adequate time to control vehicle, and frequently the unstable motions may become worse if the driver reacts improperly [9].

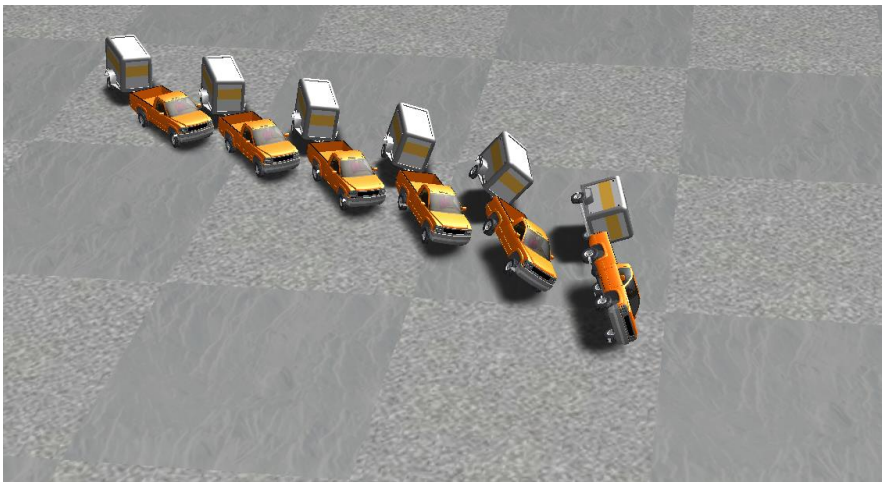

Figure 1-5. The roll-over of a CT combination

According to National Highway Traffic Safety Administration (NHTSA) and Fatality Analysis Reporting System (FARS), there were 2,792 trailer-related fatal accidents in the United States in 2014, and they killed more than 3,670 people. Trailers were involved in more than 8 percent of all fatal accidents that year [55].

In order to prevent the fatal accidents and improve the stability of CT combinations, various stability control systems have been developed and implemented recently [15]. For example, variable geometry approach (VGA), active rear steering (ARS), active trailer braking and active torque vectoring (ATV) were investigated by many researchers [5-6, 16]. To design active safety systems (ASSs), various car-trailer models with a different number of degrees of freedom (DOF) were developed, such as a multiple DOF CT model developed using CarSim commercial software [11, 17-18]. However, the parameters of CT combinations and operating conditions are frequently assumed to be invariant in the design of controllers. In reality, physical parameters may be uncertain or difficult to measure. An ASS designed without accurate vehicle parameters may exhibit poor robustness. This inspirits compelling motivations to develop and analyze CT system models and to design robust active trailer differential braking (ATDB) controller to improve lateral stability of CT combinations.

1.3 Thesis Contributions

In order to examine the fidelity, complexity, and applicability of CT models for control algorithm development and dynamic stability analysis, a reliable nonlinear CT model is generated using CarSim package, and it is applied to validate and evaluate the following two CT models developed in MATLAB: 1) a linear yaw-plane model with 3-DOF, 2) a linear yaw-roll model with 5-DOF. The eigenvalue analysis based on the linear 5-DOF yaw-roll model is conducted to evaluate the stability of a CT combination. In order to examine the effect of vehicle parameters on the stability of CT combinations, sensitivity analysis of different parameters is conducted. An ATDB controller is designed for CT combinations using the linear quadratic regulator (LQR) technique to improve stability of the vehicle systems. Another ATDB controller is developed using the H_∞ robust control technique to address the robustness issues on models with system parameter uncertainties and the robustness of the controller to external disturbances caused by wind, road irregularities, etc. To improve the performance of the ATDB controllers, a genetic algorithm (GA) is applied to find optimal control variables of the active safety systems. Numerical simulations demonstrate that the parametric study may provide a guideline for trailer design variable selections, and the proposed ATDB systems can effectively increase the safety of CT combinations.

1.4 Thesis Organization

This thesis is organized as follows. In Chapter 1, the CT combinations researched in this thesis and the typical unstable motion modes of the vehicle systems are introduced. Motivation of this research is also presented in this chapter. Chapter 2 presents the literature review on CT modelling, active safety systems and control techniques. Chapter 3 describes the modeling and validation of two CT models, i.e. the linear 3-DOF yaw-plane model and the linear 5-DOF yaw-roll model. In Chapter 4, the linear stability analysis of the CT system based on the linear 5-DOF yaw-roll model is presented. Chapter 5 introduces the ATDB controllers designed using the LQR and H_∞ robust control techniques. Chapter 6 summarizes the results of the research and provides suggestions for future work.

2.Literature Review

2.1 Introduction

This chapter conducts a comprehensive literature review on researches related to modelling of CT combinations, active safety systems (ASSs) and various control techniques. To address the stability problem of CT combinations, numerous ASSs have been developed, such as VGA, ARS and active trailer braking. Various control techniques have been used to design ASSs for CT combinations. It is found that ASSs can improve the stability of CT combinations.

2.2 Car-Trailer Modeling

In order to understand the dynamics of CT combinations and to conduct numerical simulations, various mathematical models have been developed and used. An accurate vehicle model is very important to design controllers and to analyze the dynamic behavior of CT combinations.

Ellis [19], Den and Kang [17], Hac et al. [5] and other researchers have used the linear 3-DOF yaw-plane model of CT combinations, which neglects the roll motions of the leading and trailing vehicle units. This vehicle model is extensively used to perform the lateral dynamic analysis for CT combinations. To derive the CT model, various

assumptions are made, e.g. constant forward speed and linear tire model.

Sun developed a 4-DOF yaw-plane model and a 6-DOF yaw-roll model combined with the Magic Formula tire model [11, 20]. Anderson and Kurtz built a 4-DOF model and a 6-DOF model considering longitudinal motion and aerodynamic lift and drag forces [18]. Mokhiamar [21] developed a 15-DOF nonlinear model using MATLAB/Simulink software, which includes 9-DOF for the sprung masses of the towing and towed vehicle units and 6-DOF for the wheels.

The more complex and highly nonlinear mathematical models were developed by Plöchl et al. [22] and Fratila and Darling [23]. Plöchl et al. generated a 29-DOF model considering aerodynamic forces and suspension systems with McPherson strut. Fratila and Darling developed a CT model with 24-DOF using Lagrangian approach, which takes into account a tow-ball point linkage between the car and trailer.

In order to generate more comprehensive CT models with large numbers of DOF, researchers use commercial multi-body dynamics (MBD) software packages, such as DADS (dynamic analysis and design system), CarSim, and ADAMS (automated dynamic analysis of mechanical systems). These programs automatically generate and solve the equations of motion of CT models with given constraints, forces and inputs. Sharp and Fernandez [24] generated a 32-DOF model considering 15 rigid bodies using AutoSim. Sustersic et al. [25] developed and validated a CT model using ADAMS. In this model, the aerodynamic forces obtained from a computational fluid

dynamics (CFD) simulation were included.

Generally, a highly nonlinear vehicle models is accurate to characterize the dynamics of a vehicle system. However, a simplified linear model is suitable to design controller and can improve computational efficiency of numerical simulations. It is important to apply a simplified linear model without losing the essential dynamic features of a vehicle system concerned [26].

2.3 Active Safety Systems

CT combinations are featured with unique unstable motion modes due to their complex structures, which may lead to fatal traffic accidents [27]. When driving a CT combination, it is generally difficult for a driver to sense the motion cues of the trailing unit, and driver's control input (steering, braking) is mainly based on the towing unit [15]. In order to improve the lateral stability of CT combinations, various stability control systems have been developed recently [28].

To prevent the unstable motion modes of the articulated vehicle systems, various passive systems have been developed in the past decades. For example, a four bar linkage between the towing and towed units of a CT combination has been proposed by Sorge [29]. Sharp and Fernandez [24] suggested a coulomb friction damper at the pintle pin to prevent snaking motions of the CT combination. However, it is well

reported that there are limitations of these passive systems. To address the limitations, various active control systems have been proposed. Direct yaw moment (DYM) control has been widely applied to improve vehicle lateral stability using differential braking to generate yaw moment of the system. Active steering systems have also been developed to enhance the directional performance of road vehicles.

2.3.1 Active Steering Systems

Kageyama and Nagai [30] proposed an active rear wheel steering (ARS) system and an active four wheel steering (AFS) system based on state variable feedback control to stabilize the trailer at high speeds. It is proved that compared with the ARS system, the AFS system is more effective to stabilize the CT combination.

Recently, Rangavajhula and Tsao [31] developed an active trailer steering (ATS) using the LQR technique to improve the stability of articulated heavy vehicles (AHV). A rearward amplification (RWA) ratio was used as the controller design criterion to minimize the path-following off-tracking (PFOT) value at low speeds. He and Wang [32] proposed a driver-hardware-in-the-loop (DHIL) real-time simulation platform to evaluate the performance of an ATS system designed for double-trailer articulated heavy vehicles (DTAHV). It effectively assesses the performance of the ATS system.

Even though promising results of active steering systems for articulated vehicles have been demonstrated, it is difficult to apply to the active safety systems because

steering actuators and other relevant components have to be installed.

2.3.2 Active Braking Systems

Hac et al. [5] considered the active braking control of a towing vehicle for a CT combination. The uniform braking and DYM control of the towing unit have been considered and evaluated to stabilize the snaking oscillations of the system. Experiments were performed using two trailer configurations, which correspond to the structures of double axles and single axle. Simulation results have shown that the DYM control of leading unit is more effective in stabilizing the yaw instability than the uniform braking control.

Mokhiamar and Abe [15] also introduced a DYM control system of the leading unit of a car-caravan combination. Two types of controller have been developed using side-slip control and yaw rate control based on differential braking. However, the car-caravan combination with the side-slip type of DYM control is more stable than that with the yaw rate control type of DYM.

Fernandez and Sharp [33] and Plochl et al. [22] introduced active trailer braking systems. This strategy applies individual braking of each trailer wheel to generate desired yaw moment of the system, which can eliminate the unstable motion modes of CT combinations. Both reports considered the use of nonlinear tire models to design controllers. It was reported that under a turning or lane change maneuver, the

trailer sway could be attenuated by using the active trailer braking systems.

Shamin et al. [6] compared different stability control methods based on either active trailer braking or active trailer steering (ATS). Numerical simulation results indicated that a CT combination with each of the active control systems outperformed the baseline CT combination in terms of all dynamic responses. Between the schemes of active trailer braking and ATS, the active trailer braking controller can achieve better performance in comparison with ATS method for CT combinations at high speeds.

2.3.3 Active Anti-Roll Systems

It is reported that active steering systems and active braking systems can improve the roll stability of articulated vehicles [34-35]. In order to enhance the roll stability of AHVs, active roll control (ARC) systems have been proposed [36-38]. Additional hydraulic actuators are used to apply roll moments to sprung masses of vehicles. Simulation results have shown that ARC systems can increase roll-over threshold, and thus improve the roll-over stability of AHVs.

2.4 Control Techniques

There are various control techniques introduced and implemented for the design of active safety systems for CT combinations. These techniques include the LQR control [8, 11, 26], proportional-integral-derivative (PID) control [28, 39], sliding mode

control [1, 21], H_∞ control [40], and Fuzzy Logic control [41-42].

Especially, controllers based on the LQR technique have been explored for articulated vehicles. These controllers can be designed following a systematic procedure, and they may frequently achieve superior performance as well. However, these controllers exhibit poor robustness in the presence of model parameter uncertainties, unmodeled dynamics and external disturbances. In the design of a LQR controller, it is frequently assumed that vehicle forward speed and system parameters are constant. However, in reality, trailer payload and forward speed may vary within a range. To address this problem, controllers based on the H_∞ or μ synthesis control technique are proposed. Robustness is one of important criteria in the design of controllers due to the differences between a mathematical vehicle model and an actual physical vehicle system [43]. The μ synthesis theory has successfully addressed robustness issue on models with system uncertainties and external disturbances [44-47].

2.5 Objectives of the Research

The primary objective of this thesis can be summarized as follows:

- Developing simplified linear models in the presence of nonlinear dynamics for CT combinations and validating the models using CarSim package.

- Conducting eigenvalue analysis to examine the stability of a CT combination with varying trailer parameters.
- Developing active trailer differential braking (ATDB) controllers to improve the stability of CT combinations and applying the robust μ synthesis technique to enhance the robustness of the ATDB controller.

3. Linear CT Models

3.1 Introduction

In this chapter, the linear CT models developed in the research are introduced. In the conceptual design of ASSs, the development of control strategies and the fabrication of virtual prototypes mainly depend on the model-based numerical simulations [48]. Thus, it is important to select effective dynamic CT models that are reliable and applicable for the development of ASSs. A linear 3-DOF yaw-plane model and a linear 5-DOF yaw-roll model are introduced and validated using the corresponding nonlinear CarSim model.

3.2 CT Modeling

The CT combination to be investigated in the research consists of a car and a trailer, which are connected by a hitch. For the two CT models generated in MATLAB, each axle of the vehicle units is represented by a single wheel. Based on the body fixed coordinate systems, $X-Y-Z$ and $X_1-Y_1-Z_1$, for the car and trailer, respectively, the CT models can be described in terms of the respective governing equations of motion. In the vehicle modeling, the pitch and bouncing motions and longitudinal and lateral load transfer are ignored, and the aerodynamic forces are

neglected. It is assumed that the articulated angle between the car and trailer is small, and the roll stiffness and damping coefficients of the vehicle suspension systems are constant when the roll motion is involved. Figure 3-1 illustrates the schematic representation of the car-trailer combination.

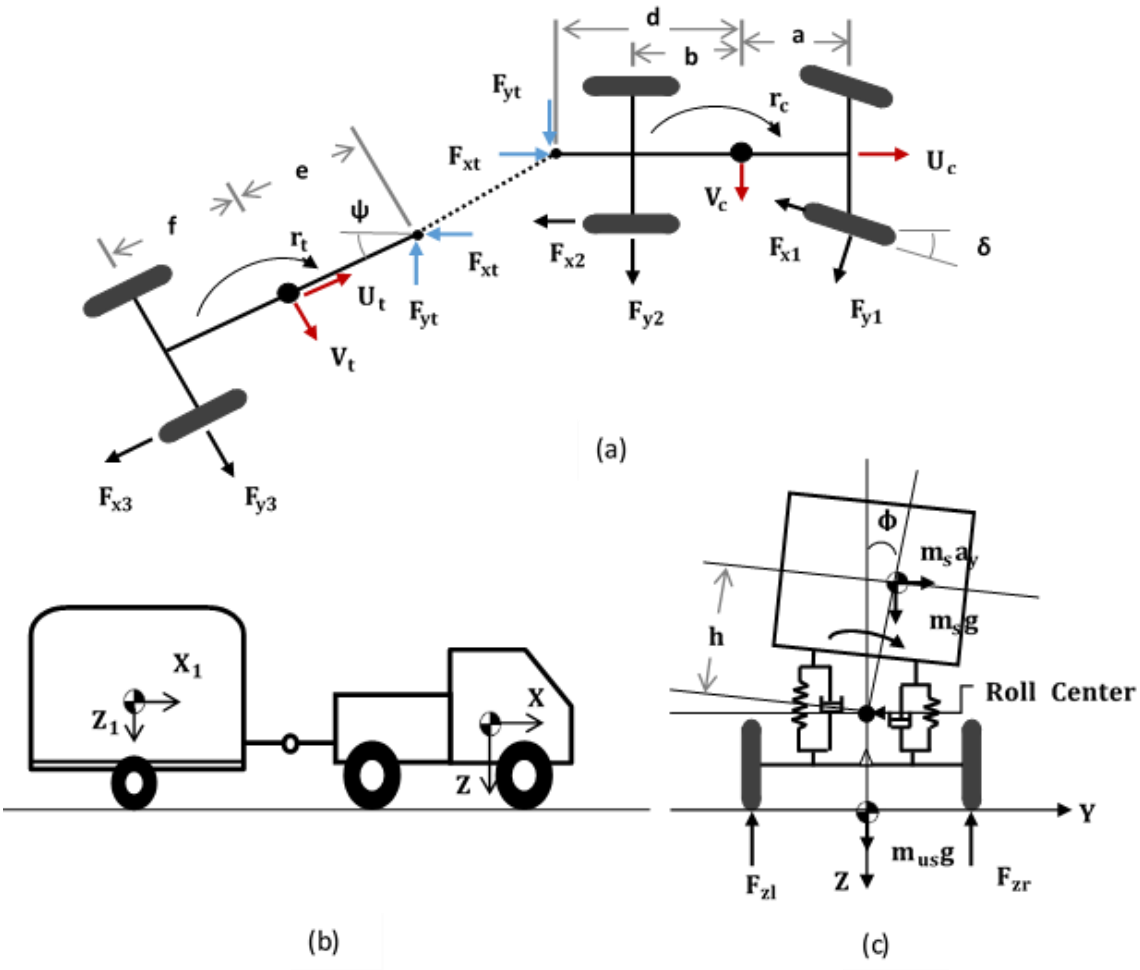

Figure 3-1. The schematic representation of the Car-trailer model: (a) top view; (b) side view; and (c) rear view

The equations of motion for the car are

$$m_c\left(\dot{U}_c - r_c \cdot V_c\right) - m_{cs} \cdot h_1 \cdot \dot{r}_c \cdot \phi_c = -F_{x1} \cdot cos(\delta) + F_{y1} \cdot sin(\delta) - F_{x2} + F_{xt} \quad (1)$$

$$m_c\left(\dot{V}_c + r_c \cdot U_c\right) + m_{cs} \cdot h_1 \cdot \ddot{\phi}_c = F_{x1} \cdot sin(\delta) + F_{y1} \cdot cos(\delta) + F_{y2} + F_{yt} \quad (2)$$

$$I_{z1} \cdot \dot{r}_c - I_{xz1} \cdot \ddot{\phi}_c = \left(F_{x1} \cdot sin(\delta) + F_{y1} \cdot cos(\delta)\right) \cdot a - F_{y2} \cdot b - F_{yt} \cdot d \quad (3)$$

$$(I_{xx1} + m_{cs} \cdot h_1^2) \cdot \ddot{\phi}_c - I_{xz1} \cdot \dot{r}_c + m_{cs} \cdot h_1 \cdot \left(\dot{V}_c + r_c \cdot U_c\right) = (m_{cs} \cdot g \cdot h_1 - kr_1) \cdot \phi_c - cr_1 \cdot \dot{\phi}_1 + F_{yt} \cdot z_1 \quad (4)$$

The equations of motion for the trailer are

$$m_t\left(\dot{U}_t - r_t \cdot V_t\right) - m_{ts} \cdot h_2 \cdot \dot{r}_t \cdot \phi_t = -F_{x3} - F_{xt} \quad (5)$$

$$m_t\left(\dot{V}_t + r_t \cdot U_t\right) + m_{ts} \cdot h_2 \cdot \ddot{\phi}_t = F_{y3} - F_{yt} \quad (6)$$

$$I_{z2} \cdot \dot{r}_t - I_{xz2} \cdot \ddot{\phi}_t = -F_{y3} \cdot f - F_{yt} \cdot e \quad (7)$$

$$(I_{xx2} + m_{ts} \cdot h_2^2) \cdot \ddot{\phi}_t - I_{xz2} \cdot \dot{r}_t + m_{ts} \cdot h_2 \cdot \left(\dot{V}_t + r_t \cdot U_t\right) = (m_{ts} \cdot g \cdot h_2 - kr_2) \cdot \phi_t - cr_2 \cdot \dot{\phi}_t - F_{yt} \cdot z_2 \quad (8)$$

The kinematic constraint between the car and trailer is given as:

$$\dot{V}_c - \dot{V}_t + z_1 * \ddot{\phi}_c - z_2 * \ddot{\phi}_t - d * \dot{r}_c - e * \dot{r}_t + U_c * r_1 - U_t * r_2 = 0 \quad (9)$$

The notation of vehicle system parameters and the corresponding nominal values are given in Appendix A.

3.2.1 Linear 5-DOF Yaw-Roll Model

For the 5-DOF model, the motions considered are: 1) the lateral velocity of the car, V_c, 2) the yaw rate of the car, r_c, 3) the roll angle of the sprung mass of the car, ϕ_c, 4)

the yaw rate of the trailer, r_t, and 5) the roll angle of the sprung mass of the trailer, ϕ_t. In the linear vehicle modeling, the following assumptions have been made: (1) the forward speed of the car (U_c) and the trailer (U_t) are the same, and they are treated as a constant, U; (2) the longitudinal forces are neglected; (3) the tire dynamic is characterized as a linear model that describes the linear relationship between the tire slip angle and the corresponding tire cornering force; and (4) car front wheel steering angle is small, and thus $cos(\delta) = 1$ and $sin(\delta) = \delta$. The liner 5-DOF yaw-roll model can be expressed in the state-space form as

$$M\{\dot{X}\} + D\{X\} + F\delta = 0 \tag{10}$$

where δ is the car front wheel steering angle, and the state variable vector is defined as

$$\{X\} = \{\phi_c \;\; \dot{\phi}_c \;\; \phi_t \;\; \dot{\phi}_t \;\; r_c \;\; r_t \;\; V_c \;\; V_t\}^T \tag{11}$$

where V_t is the lateral velocity at the center of gravity (CG) of the trailer.

The lateral tire forces F_{y1}, F_{y2} and F_{y3} can be determined using the following linear relationships between the tire slip angle and the corresponding cornering force:

$$F_{y1} = C_1.\alpha_1 \tag{12}$$

$$F_{y2} = C_2.\alpha_2 \tag{13}$$

$$F_{y3} = C_3.\alpha_3 \tag{14}$$

where C_1, C_2 and C_3 are the cornering stiffness of the car front and rear tire, and the trailer tire respectively, and α_1, α_2 and α_3 are side-slip angle of the tires. The side-slip angle can be expressed as follows:

$$\alpha_1 = \delta - \frac{V_c + a.r_c}{U} \tag{15}$$

$$\alpha_2 = \frac{b.r_c - V_c}{U} \tag{16}$$

$$\alpha_3 = \frac{f.r_t - V_t}{U} \tag{17}$$

The matrices shown in Equation (10) are provided in Appendix B.

3.2.2 Linear 3-DOF Yaw-Plane Model

The 3-DOF model is the same as the 5-DOF model except for the roll motions of the sprung mass of the car and trailer, ϕ_c and ϕ_t. In the 3-DOF model, the roll motions are neglected. In the case of the 3-DOF model, all the assumptions made are the same as those for the 5-DOF model. For the 3-DOF model, the state variable vector is defined as

$$\{X\} = \{\, r_c \;\; r_t \;\; V_c \;\; V_t\}^T \tag{18}$$

3.2.3 Nonlinear CarSim Model

In this research, a nonlinear CarSim CT model is generated to validate the linear 3-DOF and the linear 5-DOF models. In the CarSim model, the motions considered are as follows. Each of the sprung masses, car and trailer, is treated as a rigid body with 6-DOF: three translating motions along the x, y and z axes and three rotary motions around the x, y and z axes respectively. The trailer is attached to the car at the hitch point with a ball joint, which allows the trailer to rotate in roll, yaw, and pitch relative to the car [49]. The axles have roll and vertical motions. Nonlinear tire and suspension models are also taken into account. Aerodynamic forces are neglected.

3.3 Model Validation

In order to examine the fidelity of the linear 3-DOF and 5-DOF models, the nonlinear CarSim model is used as a baseline model. The 3-DOF and 5-DOF models are generated in MATLAB. To compare the dynamic responses of the two linear models with those of the CarSim model, numerical simulations are conducted under the car front wheel steering angle input of a single cycle of sine-wave with an amplitude of 0.0175 rad and a frequency of 0.318 Hz as shown in Figure 3-2 at the vehicle forward speed of: 1) 60 km/h (low-speed single lane-change maneuver), and 2) 95 km/h

(high-speed single lane-change maneuver).

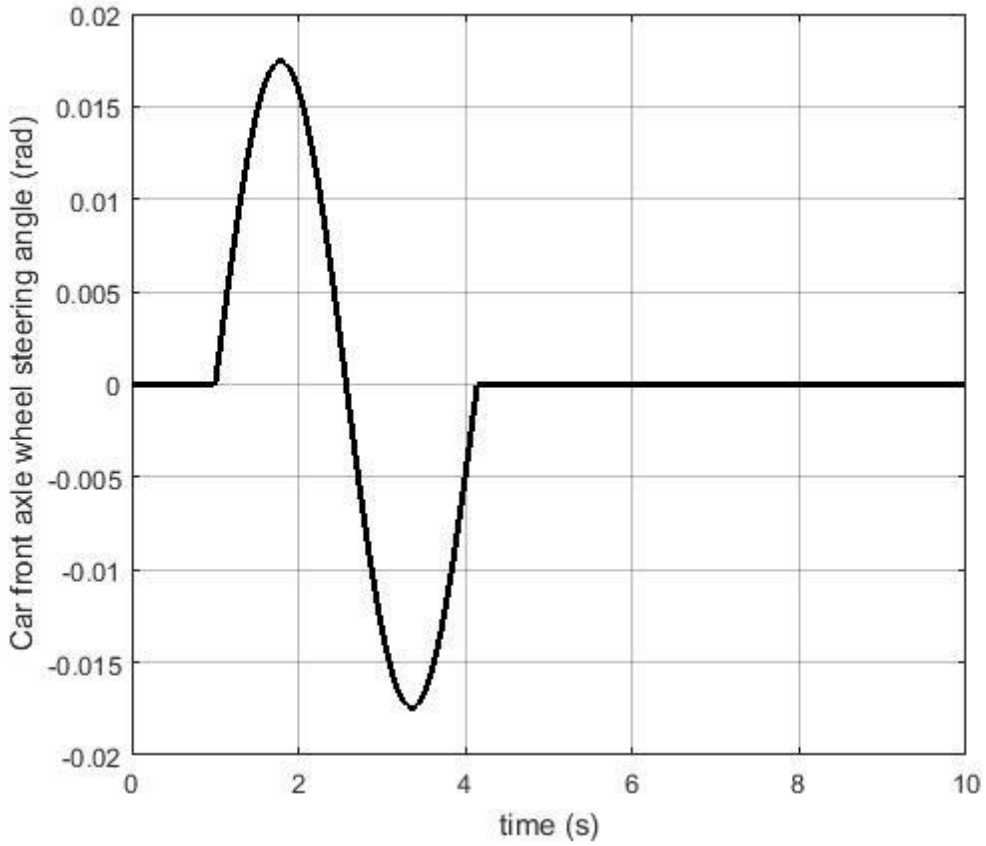

Figure 3-2. Car front axle wheel steering input for the single lane-change maneuver

3.3.1 Simulation Results under Low-Speed Maneuver

Figures 3-3 and 3-4 show the time history of the lateral acceleration at the CG of the car and the trailer for the 3-DOF, 5-DOF, and the CarSim models. As shown in Figures 3-3 and 3-4, the simulation results based on the two linear models are in excellent agreement, and these results are slightly deviate from that of the CarSim model.

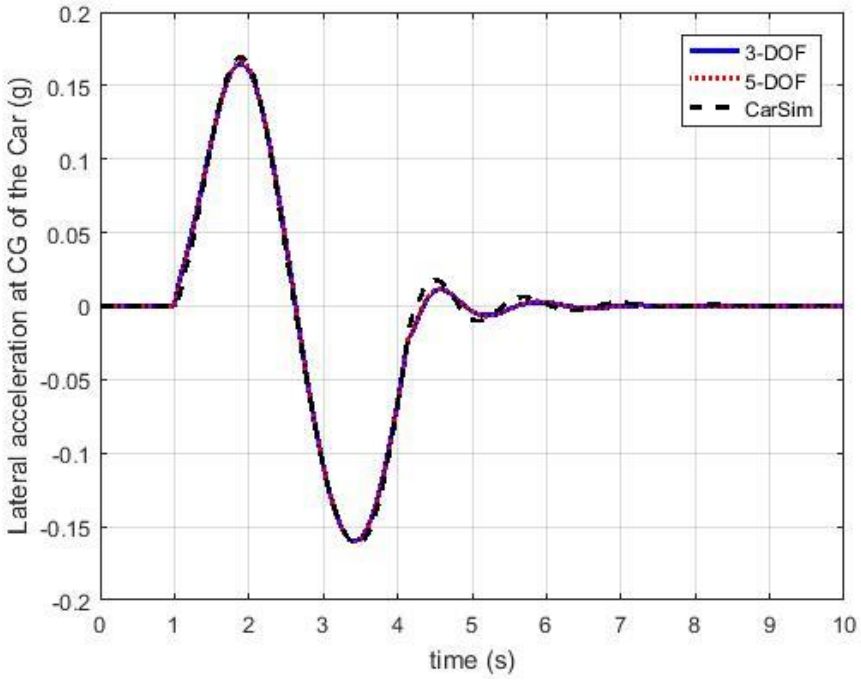

Figure 3-3. Time history of the lateral acceleration at the CG of the car for the 3-DOF, 5-DOF, and the CarSim models at the vehicle forward speed of 60 km/h

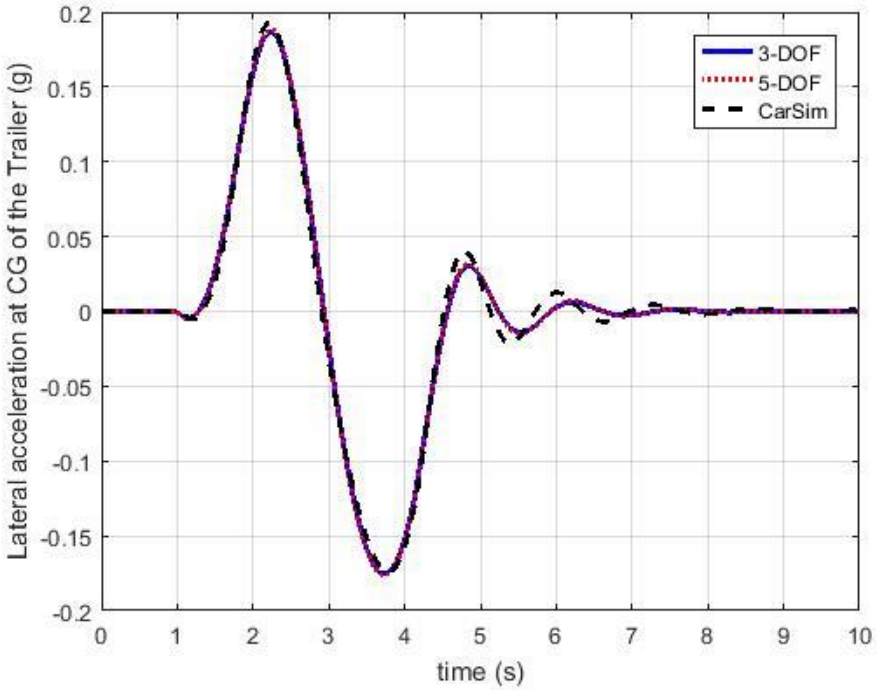

Figure 3-4. Time history of the lateral acceleration at the CG of the trailer for the 3-DOF, 5-DOF, and the CarSim models at the vehicle forward speed of 60 km/h

Table 3-1 offers the peak values of the lateral acceleration at the CG of the car and trailer shown in Figures 3-3 and 3-4. If the simulation results based on the CarSim model are treated as the reference data, the relative errors of the results for the 3-DOF or 5-DOF model with respect to the CarSim model can be calculated. The relative errors are also listed in Table 3-1. In the case of the lateral acceleration at the CG of the car, the maximum relative error of the linear models with respect to the CarSim model is 2.6 % (absolute value). In the case of the lateral acceleration at the CG of the trailer, the maximum relative error of the linear models is 3.22 % (absolute value).

Table 3-1. The peak lateral acceleration at the CG of the vehicle units for the 3-DOF, 5-DOF, and the CarSim models

	Positive peak lateral acceleration at the CG of the car (g)	Negative peak lateral acceleration at the CG of the car (g)	Positive peak lateral acceleration at the CG of the trailer (g)	Negative peak lateral acceleration at the CG of the trailer (g)
CarSim model	0.1694	-0.1616	0.1927	-0.1743
3-DOF model	0.165	-0.1599	0.1865	-0.1754
Relative error	-2.6 %	-1.05 %	-3.22 %	0.63 %
5-DOF model	0.166	-0.1604	0.1885	-0.1761
Relative error	-2.0 %	-0.74 %	-2.18 %	1.03 %

The time history of the yaw rates of the car and trailer of the three models are presented in Figures 3-5 and 3-6. As shown in the two figures, the simulation results based on the two linear models are almost identical. Compared with the linear models, in the case of the CarSim model, the time history of the yaw rate of the car and trailer has slightly higher peak values except for the positive peak value of the trailer for 3-DOF.

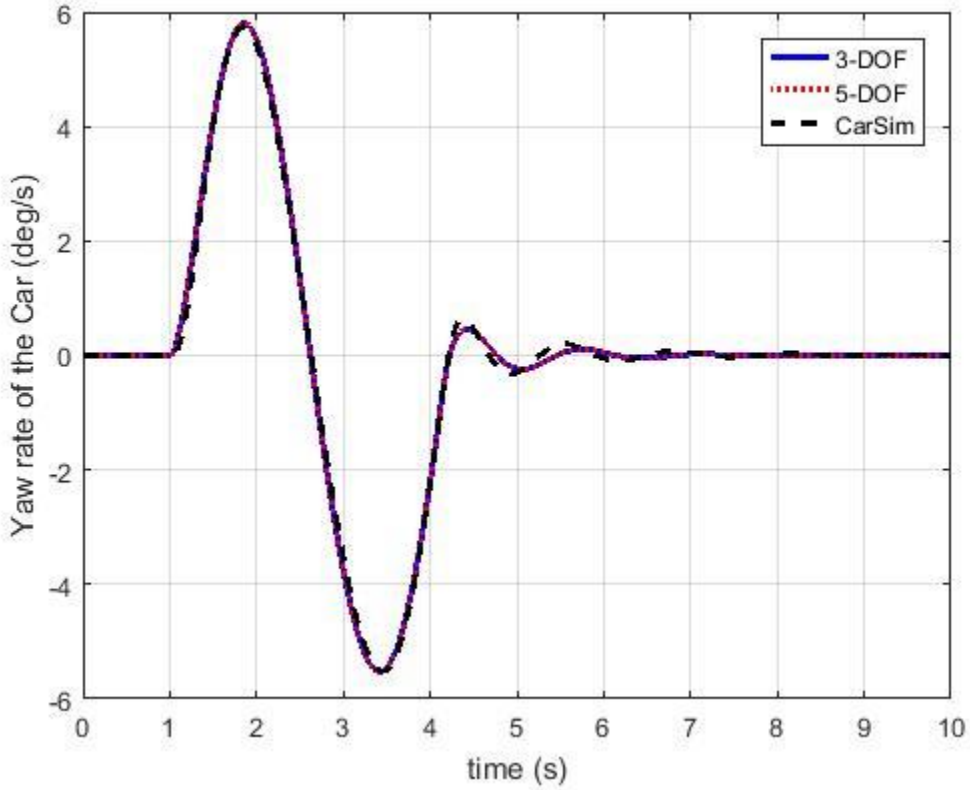

Figure 3-5. Time history of the yaw rate of the car for the 3-DOF, 5-DOF, and the CarSim models at the vehicle forward speed of 60 km/h

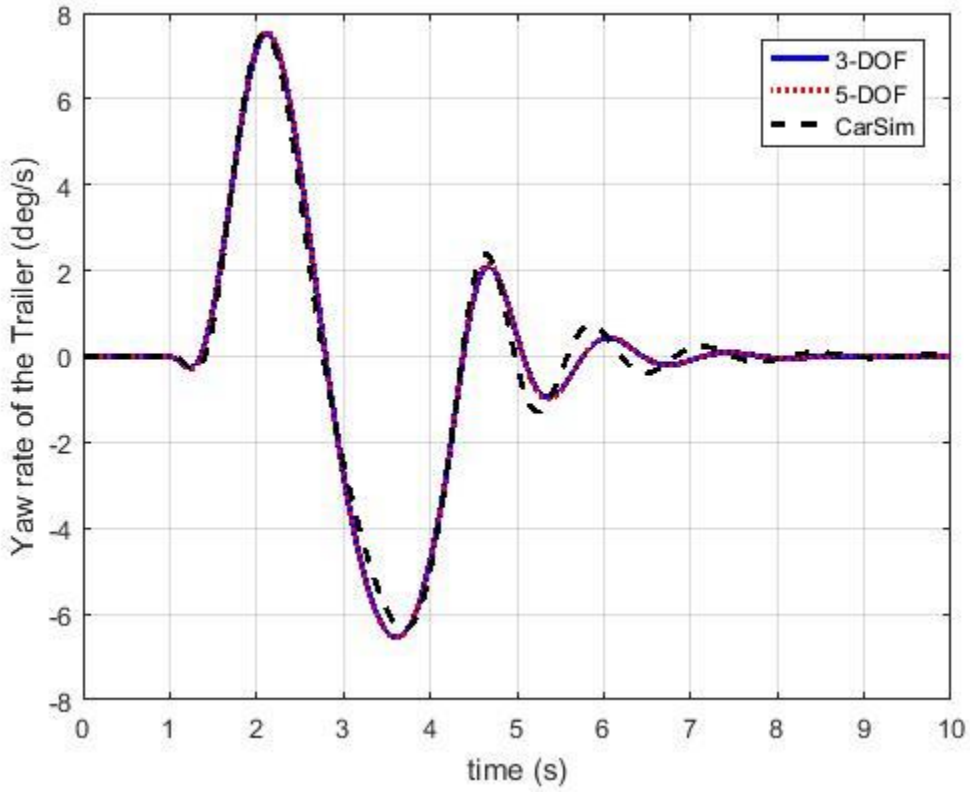

Figure 3-6. Time history of the yaw rate of the trailer for the 3-DOF, 5-DOF, and the CarSim models at the vehicle forward speed of 60 km/h

Table 3-2 lists the peak values of the yaw rate of the car and trailer. It is observed that for the peak values of the yaw rate of the vehicle units, the maximum relative error of the linear models with respect to the CarSim model is 3.1 % (absolute value).

Table 3-2. The peak yaw rate of the vehicle units for the 3-DOF, 5-DOF, and the CarSim models

	Positive peak yaw rate of the car (deg/s)	Negative peak yaw rate of the car (deg/s)	Positive peak yaw rate of the trailer (deg/s)	Negative peak yaw rate of the trailer (deg/s)
CarSim Model	5.733	-5.515	7.53	-6.355
3-DOF model	5.801	-5.528	7.493	-6.547
Relative error	1.19 %	0.24 %	-0.49 %	3.02 %
5-DOF model	5.808	-5.525	7.569	-6.552
Relative error	1.31 %	0.18 %	0.52 %	3.1 %

Figures 3-7 and 3-8 illustrate the time history of the sprung mass roll angles of the car and trailer based on the numerical simulations of the 5-DOF and the CarSim models. In the case of the car sprung mass roll angle, the simulation result for the 5-DOF model slightly deviates from that for the CarSim model in the positive peak area. In the case of the trailer sprung mass roll angle, the simulation results for both models are in good agreement except for the positive peaks, which is similar to the case of roll angle of the car.

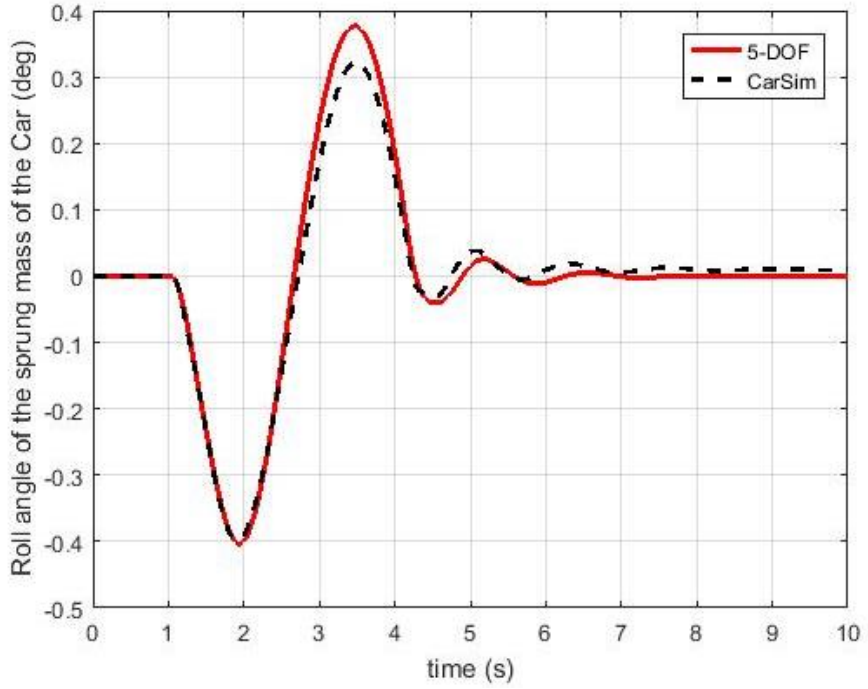

Figure 3-7. Time history of the roll angle of the car sprung mass for the 5-DOF and the CarSim models at the vehicle forward speed of 60 km/h

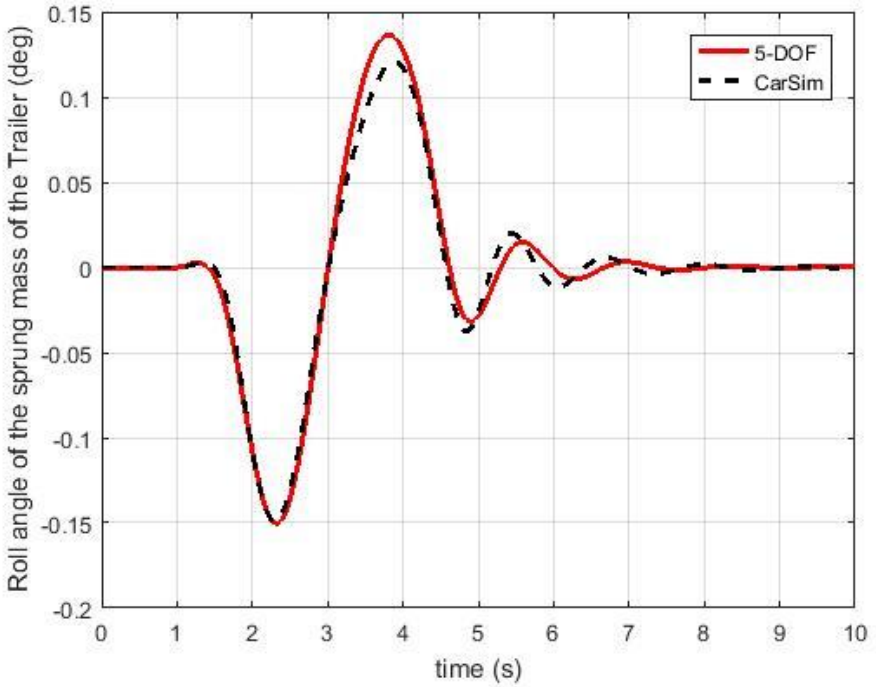

Figure 3-8. Time history of the roll angle of the trailer sprung mass for the 5-DOF, and the CarSim models at the vehicle forward speed of 60 km/h

Table 3-3 provides the peak values of the sprung mass roll angle of the car and trailer for both the 5-DOF and the CarSim models. As mentioned above, in the case of the sprung mass roll angle of the car and trailer, the simulation results for the two models match well, between which the relative error of the negative values are as low as 1.23 % and 0.6 %, respectively. However, in the case of the positive peaks of the sprung mass of the car and trailer, the relative errors are 16.8 % and 12.9 %, respectively. The main reason for the difference of the simulation results between the 5-DOF and CarSim models may result from the different suspension model used. For the linear 5-DOF model, roll spring stiffness and damping coefficients of the vehicle suspension systems are constant, while CarSim model used the nonlinear suspension model.

Table 3-3. The peak roll angle values of the sprung mass of the car and trailer for the 5-DOF and CarSim models

	Positive peak roll angle of the sprung mass of the car (degree)	Negative peak roll angle of the sprung mass of the car (degree)	Positive peak roll angle of the sprung mass of the trailer (degree)	Negative peak roll angle of the sprung mass of the trailer (degree)
CarSim Model	0.3226	-0.3982	0.1208	-0.1494
5-DOF model	0.3768	-0.4031	0.1364	-0.1503
Relative error	16.8 %	1.23 %	12.9 %	0.6 %

The aforementioned simulation result comparison indicates that under the low-g single lane-change maneuver, the 3-DOF, 5-DOF, and the CarSim models are in very good agreement in terms of the time histories of the lateral acceleration and the yaw rate of the car and trailer. Moreover, the 5-DOF and the CarSim models reach good agreement in terms of the time histories of the sprung mass roll angle of the car and the trailer.

3.3.2 Simulation Results under High-Speed Maneuver

Figures 3-9 to 3-14 illustrate simulation results of the 5-DOF and the CarSim models under the high-speed maneuver in terms of the time history of the car lateral acceleration, trailer lateral acceleration, car yaw rate, trailer yaw rate, car roll angle, and trailer roll angle, respectively. Unlike the results shown in Figures 3-3 to 3-8 for the low-speed maneuver at the speed of 60 km/h, under the high-speed maneuver at the vehicle forward speed of 95 km/h, the simulation results based on the 5-DOF model give different shape of the peaks and oscillation deviated from the CarSim model. However, the overall phenomena are quite similar between two models. The reason for this difference is that the linear 5-DOF model and CarSim model use different tire models. The cornering stiffness of the linear model is constant so that the lateral tire force can increase continuously without tire force saturation. But the nonlinear tire model is saturated with a large tire side-slip angle.

The simulation results shown in Figures 3-9 to 3-14 imply that under the high-speed single lane-change maneuver, the linear 5-DOF model could be used to design ATDB controller for the CT combination.

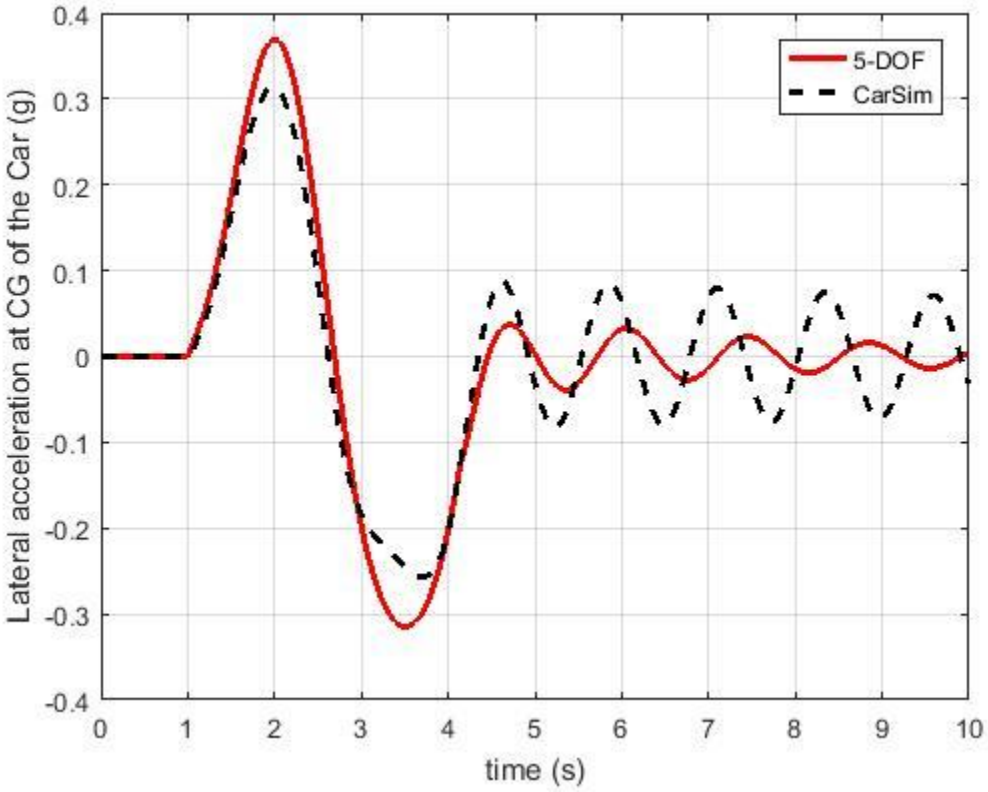

Figure 3-9. Time history of the lateral acceleration at the CG of the car for the 5-DOF and the CarSim models at the vehicle forward speed of 95 km/h

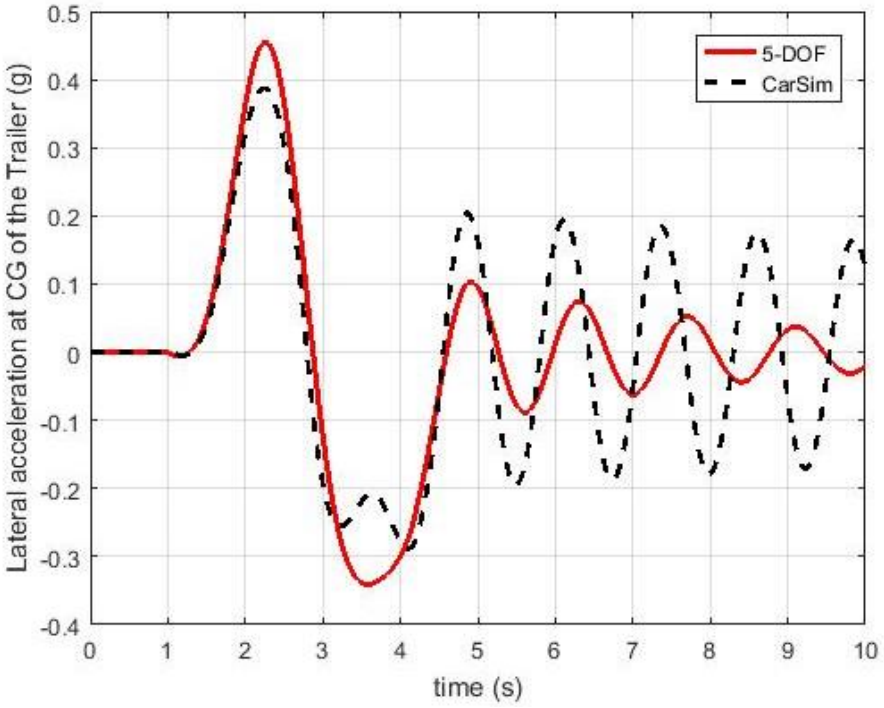

Figure 3-10. Time history of the lateral acceleration at the CG of the trailer for the 5-DOF and the CarSim models at the vehicle forward speed of 95 km/h

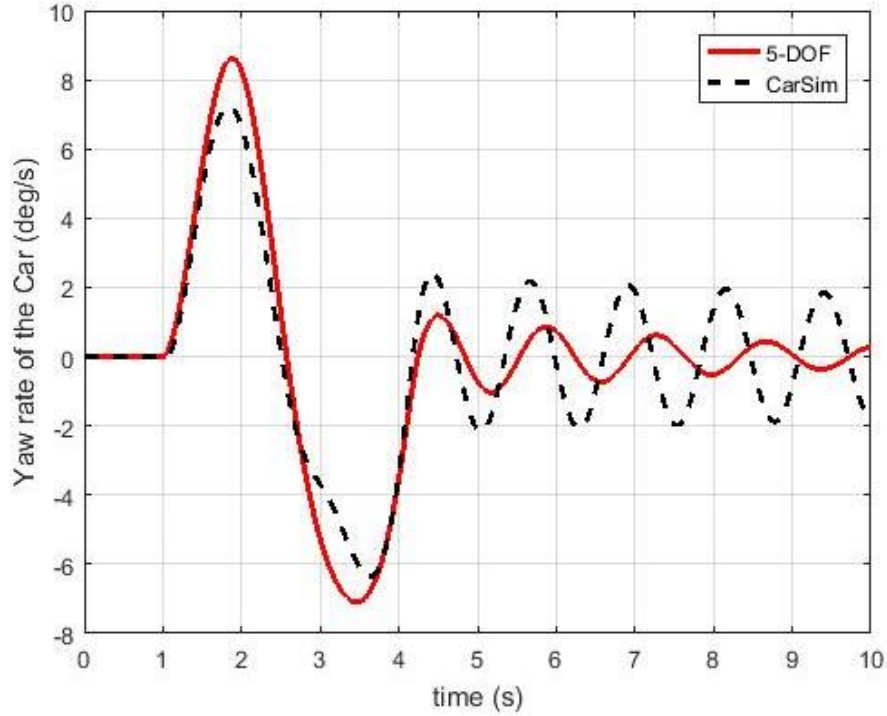

Figure 3-11. Time history of the yaw rate of the car for the 5-DOF and the CarSim models at the vehicle forward speed of 95 km/h

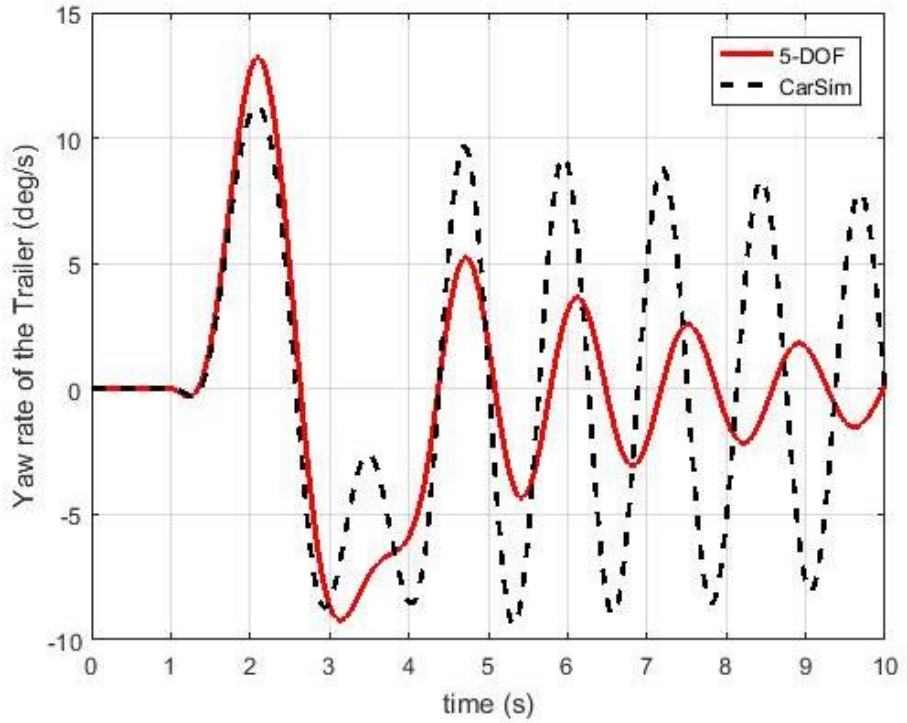

Figure 3-12. Time history of the yaw rate of the trailer for the 5-DOF and the CarSim models at the vehicle forward speed of 95 km/h

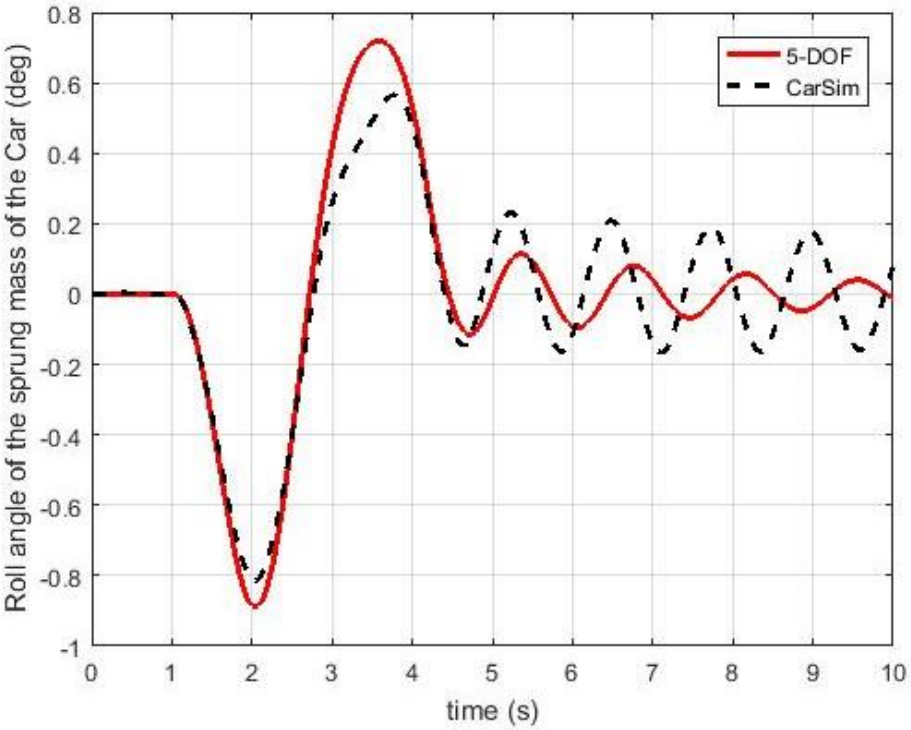

Figure 3-13. Time history of the roll angle of the car sprung mass for the 5-DOF and the CarSim models at the vehicle forward speed of 95 km/h

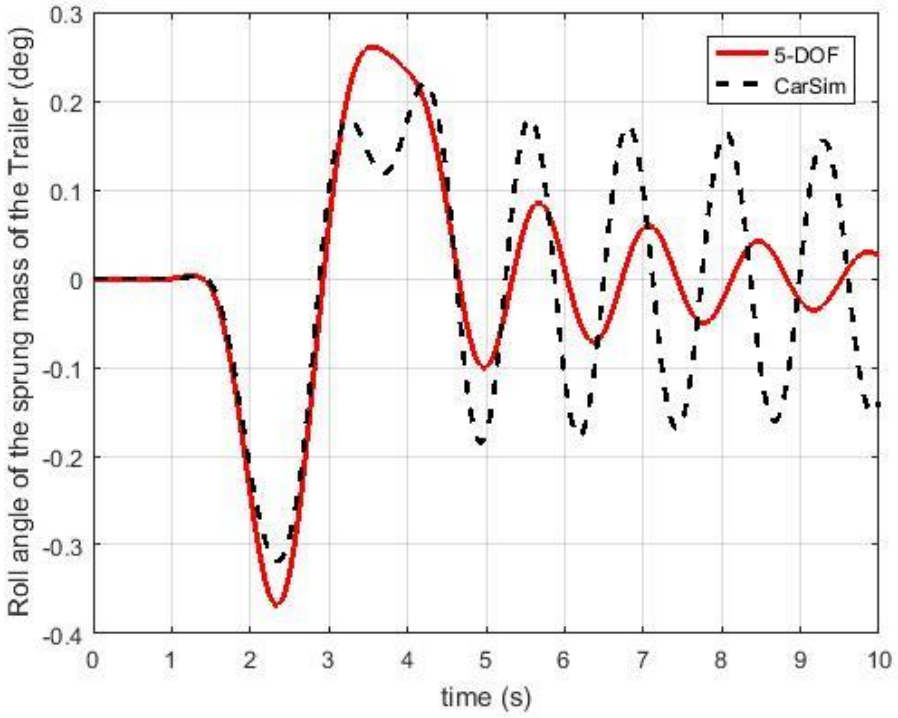

Figure 3-14. Time history of the roll angle of the trailer sprung mass for the 5-DOF and the CarSim models at the vehicle forward speed of 95 km/h

3.4 Summary

In this chapter, the following two models are generated in MATLAB to represent a CT combination: 1) a linear yaw-plane model with 3-DOF, and 2) a linear yaw-roll model with 5-DOF. The two CT models are compared and validated using a nonlinear yaw-roll model developed in CarSim software. In order to carry out the benchmark investigation, typical single lane-change maneuvers at low and high speeds are simulated. The following observations can be made from the benchmark

investigation:

- Under low-speed (60 km/h) single lane-change maneuvers, the linear models and the CarSim model are in good agreement;
- Under high-speed (95 km/h) single lane-change maneuvers, the tire cornering force saturation occurs, and the linear models can't simulate the nonlinear dynamic characteristics of CT combinations. But overall phenomena are quite similar between the linear 5-DOF model and CarSim model.

4. Stability Analysis

4.1 Introduction

In this chapter, stability of the CT combination is investigated using the 5-DOF model described in the previous chapter. In order to study the inherent dynamic stability characteristics, eigenvalue analysis based on the linear 5-DOF yaw-roll model is conducted. This chapter also performs the sensitivity analysis of different parameters, e.g. trailer center of gravity (CG) position, trailer mass, trailer yaw inertia, and trailer axle position, to examine the effect of vehicle parameters on the stability of CT combinations, and eventually to design an effective stability controller for the vehicles [50].

4.2 Eigenvalue Analysis

In order to estimate the unstable motion modes and predict the critical speeds of the CT combination, an eigenvalue analysis is conducted. Note that the critical speed is a maximum stable forward speed, above which the system will loss stability. The liner 5-DOF yaw-roll model can be expressed in the state-space form given in Eq. (10) and the system matrix A can be obtained from Eq. (19).

$$A = -M^{-1} \cdot D \tag{19}$$

In order to find the eigenvalues of the system matrix A, characteristic equations of the matrix can be derived. If a linear dynamic system has a complex pair of eigenvalue as

$$s_{1,2} = R_e \pm j\omega_d \tag{20}$$

where R_e and ω_d are the real and imaginary part of the eigenvalue, respectively, then the corresponding damping ratio is defined as

$$\xi = \frac{-R_e}{\sqrt{R_e^2 + \omega_d^2}} \tag{21}$$

For the linear 5-DOF yaw-roll model, the baseline values of the vehicle system parameters are listed in Appendix A. Note that the notation of the geometric parameters of the CT combination is also defined in Figure 3-1. With the given parameters of the linear model listed in Appendix A, for an eigenvalue, the damping ratio expressed in Eq. (21) is a function of the vehicle forward speed. Figure 4-1 shows the relationship between the damping ratio for each of the four motion modes and the vehicle forward speed. The vehicle becomes unstable if a damping ratio takes a negative value. The closer a curve of damping ratio versus forward speed approaches to the zero damping line, the closer the vehicle becomes unstable. Figure 4-1 doesn't show whether an unstable motion mode is related to roll or yaw motion, but the eigenvalue analysis of the linear 5-DOF yaw-roll model is very useful to estimate the instability of the CT system at different forward speeds.

Figure 4-1 indicates that within the given forward speed range, motion modes 1, 3 and 4 are stable. However, the curve of damping ratio versus forward speed for motion mode 2 intersects with the zero damping ratio line at the speed of 31.7 m/s (marked with a red circle), above which the damping ratio of mode 2 becomes negative. Thus, for mode 2, the speed of 31.7 m/s is the critical speed, above which the CT combination will lose its stability. As shown in Figure 4-1, for motion mode 2, the damping ratio decrease as the vehicle forward speed increases. It implies that the stability of the CT combination decreases with the increase of vehicle forward speed.

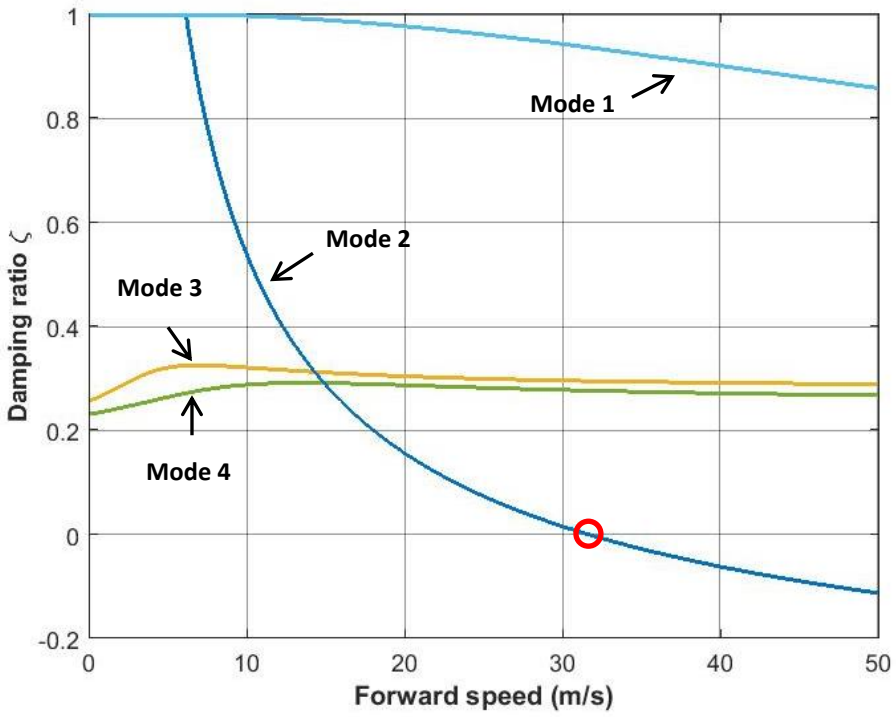

Figure 4-1. Mode damping ratios versus forward speed for the case of baseline parameter set

In order to validate the critical speed and identify the motion mode of the instability, a corresponding nonlinear CT model was developed in CarSim. Figure 4-2 shows the respective unstable motion mode of the CarSim model, which is the unstable motion mode of trailer swaying, and the corresponding critical speed is approximately 27.7 m/s. There exists a difference between the critical speed (31.7 m/s) simulated by the linear 5-DOF model and that (27.7 m/s) predicted by the nonlinear CarSim model. This difference may be resulted from the different tire modes used by the linear and nonlinear CT models. Under high-speed maneuvers, tire cornering force saturation occurs as explained in Chapter 3.

Figure 4-2. Unstable motion mode of the nonlinear CarSim model at 27.7 m/s

4.3 Effects of Trailer Parameters on the Stability of CT Combinations

The damping ratio defined in Eq. (21) is used as a measure to examine effects of typical trailer parameters on the stability of the CT combination. In order to assess the sensitivity of trailer parameters on the stability of the CT combination, only one parameter will be changed at a time.

4.3.1 Effect of Trailer Center of Gravity Position

To examine the effect of trailer center of gravity (CG) position (in the longitudinal direction) on the stability of the CT combination, the distance between the trailer CG and the hitch, *e*, is varied, while other parameters remain unchanged. It is assumed that the distance between the trailer axle and the hitch is fixed, that is, $e + f = 2.6\ m$. Thus, once *e* varies, *f* should also change accordingly. When *e* takes the values of 1.7 *m* and 2.3 *m*, the corresponding simulation results are shown in Figures 4-3 and 4-4 in terms of the damping ratios of the motion modes versus the vehicle forward speed. From Figures 4-3 and 4-4, the respective critical speeds (marked with red circles) can be determined. Table 4-1 lists the critical speeds and the values of the parameters for determining the trailer CG position for the two cases. For the purpose of comparison, the corresponding values for the baseline case (as shown in Figure 4-1) are also listed in the table. It is found that the shorter the distance between the trailer CG and the hitch, the higher the critical speed. The Trailer longitudinal CG position is directly

related to the hitch tongue load. The simulation results shown in Table 4-1 imply that a larger tongue load of the hitch (i.e., the shorter distance between the trailer CG and the hitch) be beneficial for improving the stability of the CT combination.

Table 4-1. Trailer longitudinal CG positions and critical speeds

	Baseline (e=2.0 m, f=0.6 m)	CG position (e=1.7 m, f=0.9 m)	CG position (e=2.3 m, f=0.3 m)
Critical speed (m/s)	31.7	Over 50	24

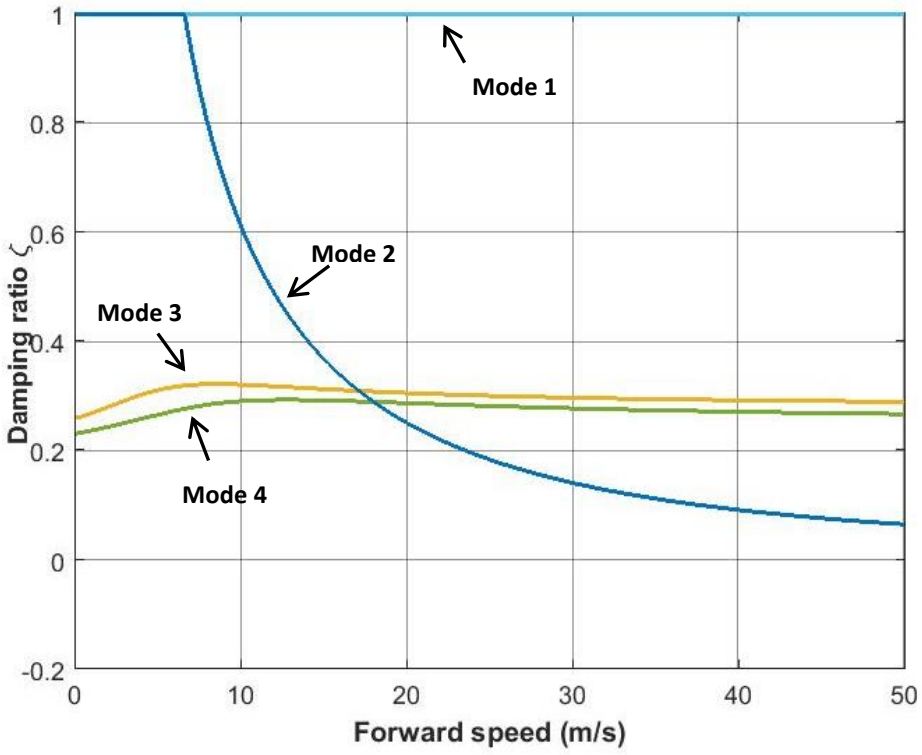

Figure 4-3. Mode damping ratios versus forward speed for the case of the trailer longitudinal CG position with e=1.7 m and f=0.9 m

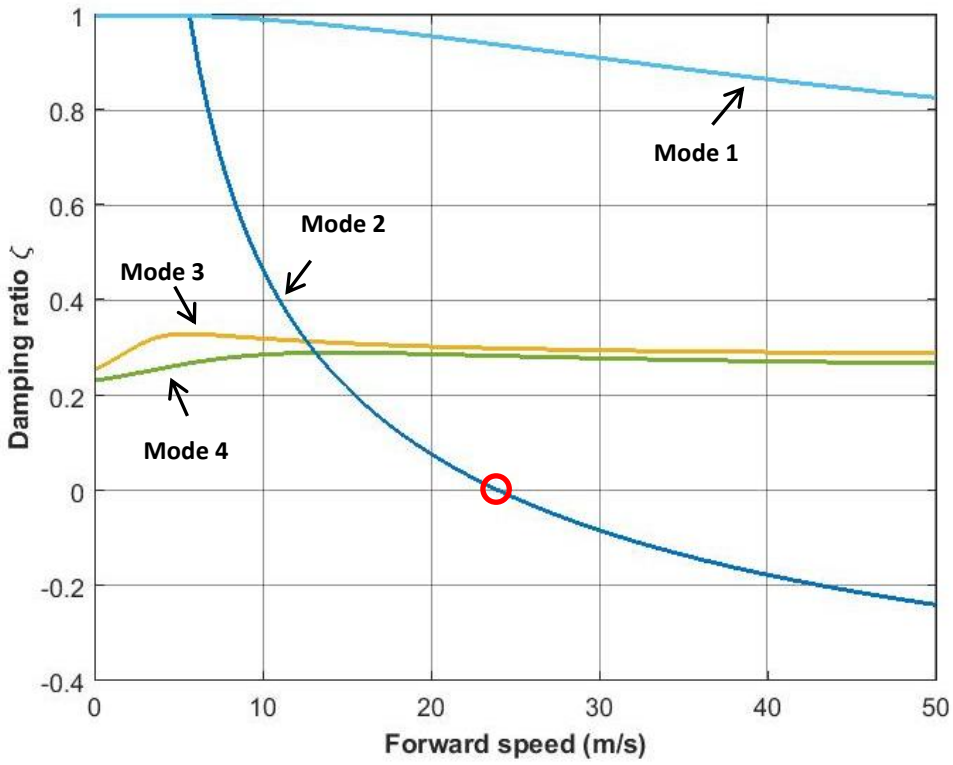

Figure 4-4. Mode damping ratios versus forward speed for the case of the trailer longitudinal CG position with *e=2.3 m* and *f*=0.3 *m*

4.3.2 Effect of Trailer Yaw Moment of Inertia

To evaluate the effect of trailer yaw moment of inertia I_{z2} on the lateral stability of the CT combination, this parameter is varied, while keeping other parameters as constants. As shown in Appendix A, the nominal value of the trailer yaw moment of inertia I_{z2} takes the value of 1,764 kgm^2, and the corresponding critical speed is 31.7 *m/s* as shown in Figure 4-1. If I_{z2} takes the values of 1,264 kgm^2 (decreasing by 28.34% from the nominal value) and 2,264 kgm^2 (increasing by 28.34% from the

nominal value), the corresponding simulation results in terms of motion mode damping ratios versus forward speed are illustrated in Figures 4-5 and 4-6, showing the critical speeds (marked with red circles) of 49.3 m/s and 25.5 m/s, respectively. Table 4-2 shows the values of the trailer yaw moment inertia and the corresponding critical speeds of the CT combination together with the baseline values. Simulation results indicate that the critical speed decreases with the increase of the trailer yaw moment of inertia.

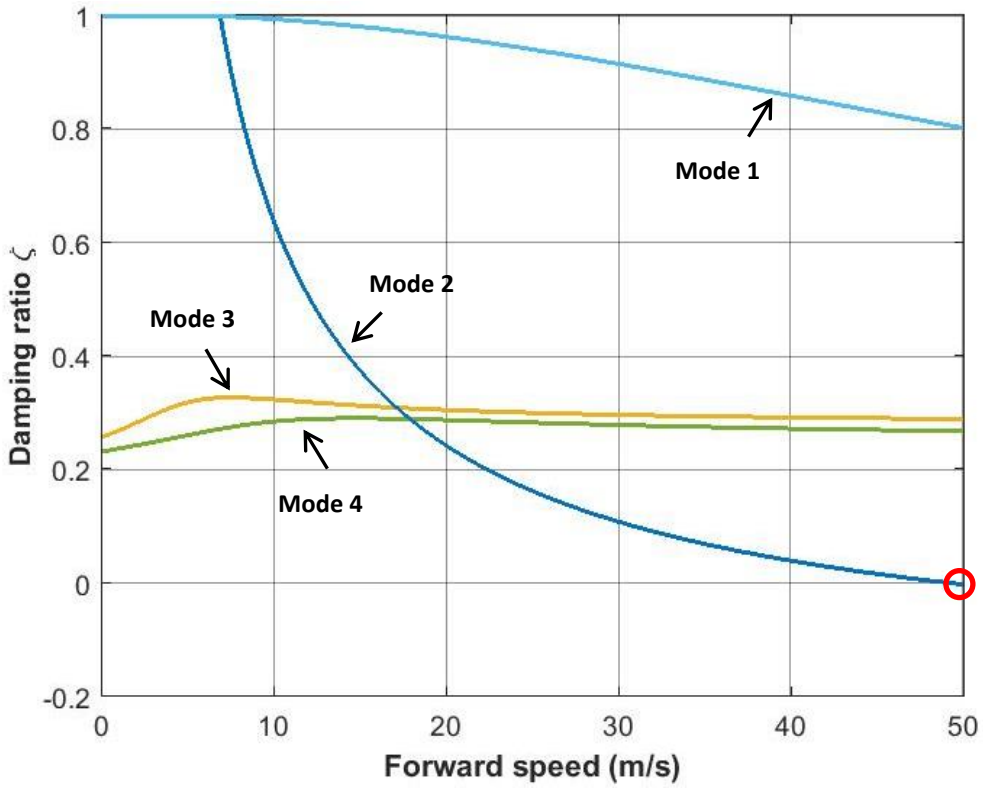

Figure 4-5. Mode damping ratios versus forward speed for the case of the trailer yaw inertia with I_{z2} = 1,264 kgm^2

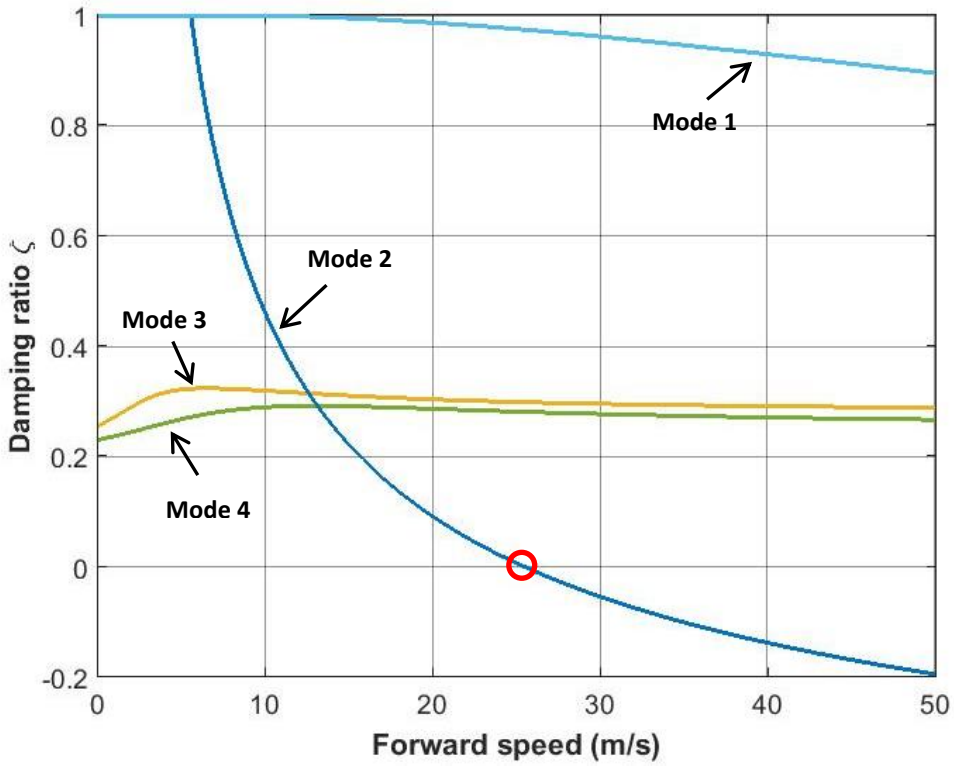

Figure 4-6. Mode damping ratios versus forward speed for the case of the trailer yaw inertia with I_{z2} = 2,264 kgm^2

Table 4-2. Trailer yaw moments of inertia and critical speeds

	Baseline (1,764 kgm^2)	Trailer Yaw Moment Inertia (1,264 kgm^2)	Trailer Yaw Moment Inertia (2,264 kgm^2)
Critical Speed (m/s)	31.7	49.3	25.5

4.3.3 Effect of Trailer Axle Position

In order to test the effect of the trailer axle position, i.e., the distance between the trailer axle and the hitch, on the stability of the CT combination, a sensitivity analysis is conducted. As shown in Figure 3-1, this distance is the defined as the addition of the distance between the trailer CG to the hitch (e) and that between the CG and the trailer axle (f). In the sensitivity analysis, the values of f and other parameters are fixed, while e takes the values of 1.5 m and 3.0 m, and Figures 4-7 and 4-8 illustrate the simulation results in terms of the damping ratios of motion modes versus forward speed. Table 4-3 lists the values of the distance between the trailer axle and the hitch and the respective critical speeds. The results shown in Table 4-3 indicate that the longer the distance, the higher the critical speed. The sensitivity analysis discloses that increasing the distance between the trailer axle and the hitch is advantageous to the improvement of the stability of the CT combination.

Table 4-3. Distances between the trailer axle and the hitch and critical speeds

	Baseline (2.6 m)	Trailer Axle Position (2.1 m)	Trailer Axle Position (3.6 m)
Critical Speed (m/s)	31.7	25.4	50

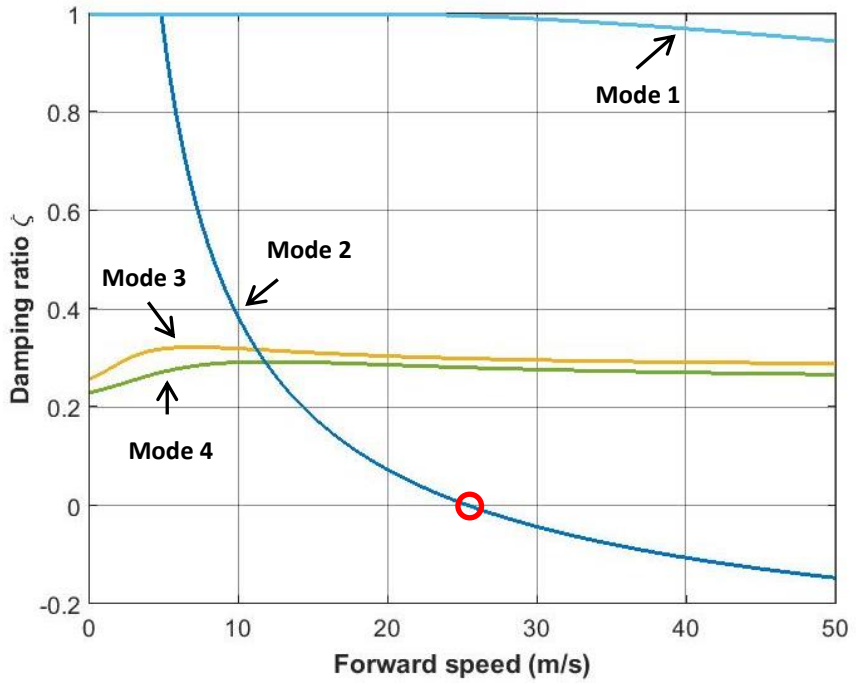

Figure 4-7. Mode damping ratios versus forward speed for the case of the distance between the trailer axle and the hitch taking the value of 2.1 *m*

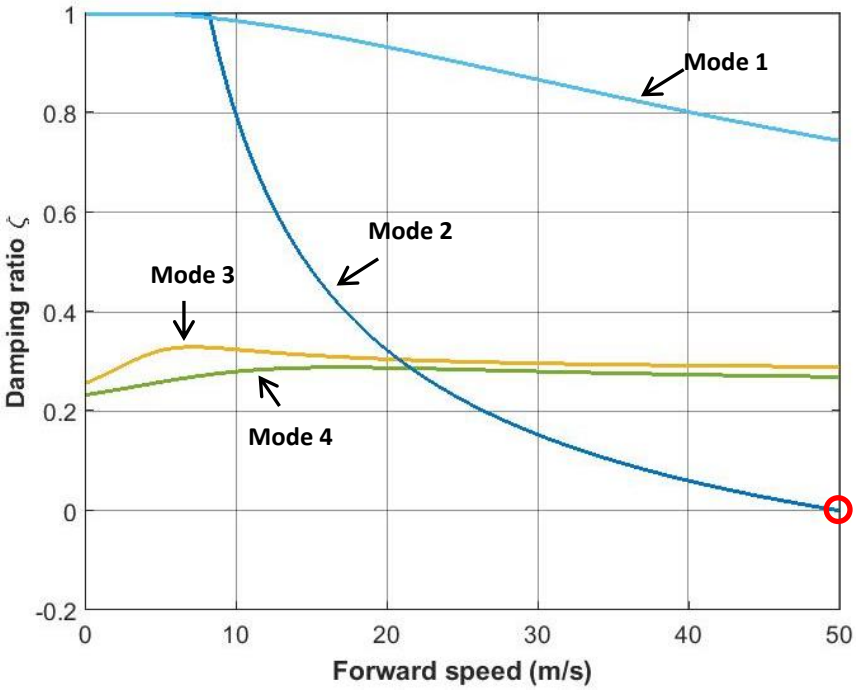

Figure 4-8. Mode damping ratios versus forward speed for the case of the distance between the trailer axle and the hitch taking the value of 3.6 *m*

4.3.4 Effect of Trailer Sprung Mass

In order to study the effect of trailer sprung mass on the CT system stability, the relationship between the damping ratios and vehicle forward speed of the least damped motion modes is investigated with different trailer sprung masses while other parameters taking their nominal values listed in Appendix A. Figures 4-9 and 4-10 show the simulation results in terms of the damping rations of the motion modes versus vehicle forward speed when the trailer sprung mass takes the values of 260 kg and 660 kg, respectively. As shown in 4-9 and 4-10, the critical speeds (marked with red circles) are 31.6 m/s and 35.5 m/s, respectively. Table 4-4 lists the values of the trailer sprung mass and the corresponding critical speeds together with the result for the baseline CT combination. Simulation results indicate that the trailer mass does not have a significant effect on the CT combination stability. Generally, higher trailer sprung mass leads to more stable responses. This phenomenon may be interpreted by the fact that a larger trailer sprung mass will cause a heavier hitch tongue load, thereby leading to a higher critical speed.

Table 4-4. Values of trailer sprung mass and critical speed

	Baseline (466 kg)	Trailer Sprung Mass (260 kg)	Trailer Sprung Mass (660 kg)
Critical Speed (m/s)	31.7	31.6	35.5

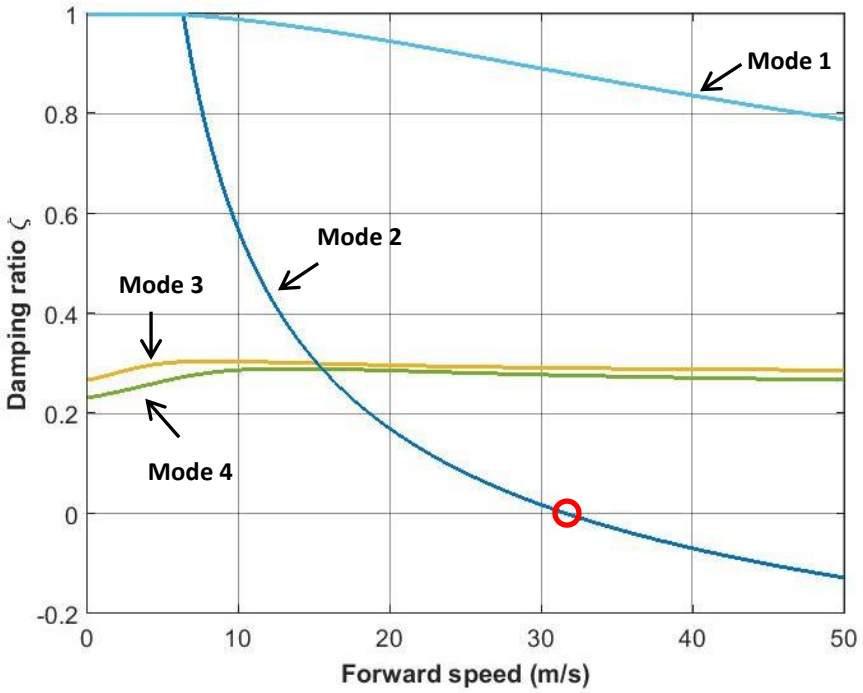

Figure 4-9. Mode damping ratios versus forward speed for the case of the trailer sprung mass with m_{2s} = 260 kg

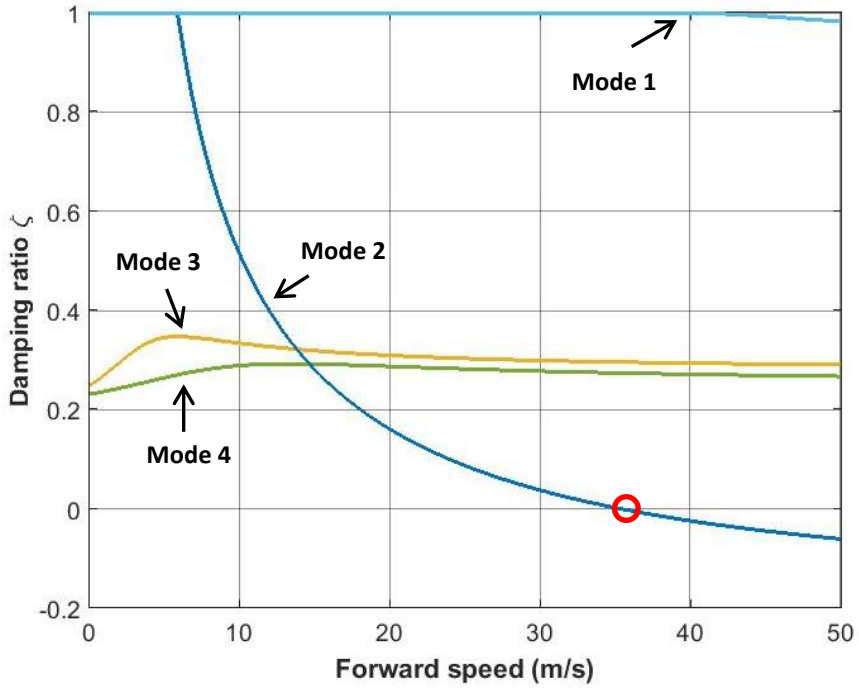

Figure 4-10. Mode damping ratios versus forward speed for the case of the trailer sprung mass with m_{2s} = 660 kg

4.4 Summary

In the chapter, the eigenvalue analysis is conducted to examine the stability of a CT combination with varying trailer parameters. It was found that different trailer parameters have varied effects on the stability of the system. Simulation results conducted in the chapter indicate that:

(1) decreasing the distance between the trailer CG and the hitch (i.e., increasing the tongue load of the hitch) is advantageous for improving the stability of the CT system;

(2) reducing trailer yaw inertia is beneficial for enhancing the stability of the CT system;

(3) increasing the distance between trailer axle and hitch causes the increasing the yaw damping effect of the trailer, leading to the stability improvement of the CT system; and

(4) Increasing trailer sprung mass has marginal positive effect on the stability of the CT combination.

5. ATDB Controllers Design

5.1 Introduction

This thesis presents the investigation on active trailer differential braking (ATDB) controller for CT combinations to enhance the stability of the systems. To this end, ATDB controllers have been designed using the control techniques, LQR method and H_∞ robust (i.e. μ synthesis) control technique. In order to evaluate the performance of the controllers, numerical simulations are conducted under a single lane-change maneuver.

5.2 ATDB Control

The main concept of the ATDB control is to use active yaw moment (M_z) resulting from a differential braking system of the trailer unit. Since the ATDB controllers would generate the external yaw moment in the trailer, Eq. (7) is modified with the addition term, M_z, which is considered as the control input.

$$I_{z2} \cdot \dot{r}_t - I_{xz2} \cdot \ddot{\phi}_t = -F_{y3} \cdot f - F_{yt} \cdot e + M_z \tag{22}$$

With Eq. (22), new state-space representation of the CT model can be written as

$$\{\dot{X}\} = A\{X\} + B\delta + B_c u \tag{23}$$

where,

$$u = M_z \tag{24}$$

where A is the system matrix, B is the disturbance matrix and B_c is the control matrix. The state variable vector X is the same as that for the baseline linear models. A, B and B_c matrices are provided in Appendix B.

5.3 LQR Controller

5.3.1 Controller Design

In order to enhance the stability of the CT combination, an ATDB strategy is proposed. To this end, an ATDB controller has been designed using the LQR technique based on the 5-DOF linear model.

The LQR-based ATDB controller design can be described as an optimization problem: Minimize the objective function or performance index:

$$J = \int_0^\infty (X^T(t)QX(t) + u^T(t)R\,u(t))\,dt \tag{25}$$

subject to the governing equations of motion of the linear 5-DOF yaw-roll model expressed in Eq. (23). In Eq. (25), Q and R are weighting matrices, *u(t)* is control variable that is defined as the yaw moment resulting from the ATDB system, *X(t)* is

the state variables defined as Eq. (11).

It is assumed that all uncontrollable modes are stable. Thus, the solution of the optimization problem is the active trailer yaw moment determined as

$$u(t) = -KX(t) \tag{26}$$

where K is the feedback control gain matrix.

5.3.2 Optimization

For the LQR-based controller, the weighting matrices Q and R have significant effect on the performance of the controller. The trial and error method is commonly used to determine desired weighting matrices for the objective function. However, this process is tedious and time consuming.

In order to design optimal ATDB controller, a Genetic Algorithm (GA) is introduced in this study. The GA is a powerful global optimization tool. It is a stochastic evolutionary algorithm based on the principles of natural evolution. The basic operations of the GA include: coding, selection, crossover and mutation. The goal of the GA is to minimize the cost value of the objective function expressed in Eq. (25). The overall optimization process of the ATDB controller based on the GA is shown in Figure 5-1.

In order to improve stability of the CT combination, the ATDB controller is designed to achieve the minimum yaw rate, roll angle and lateral acceleration of the CT

combination under a given single lane-change maneuver. The weighting factors in Eq. (25) are defined as Eq. (27).

$$Q = diag([q_1\ q_2\ q_3\ q_4\ q_5\ q_6\ q_7\ q_8\ ])\ ,\ R = [r] \tag{27}$$

The design optimization is to find desired values of the design variables that minimize the following objective function as

$$f_{obj} = \frac{\varphi_1}{\varphi\ {}^{p}_{1}} + \frac{\varphi_2}{\varphi\ {}^{p}_{2}} + \frac{\varphi_3}{\varphi\ {}^{p}_{3}} + \frac{\varphi_4}{\varphi\ {}^{p}_{4}} + \frac{\varphi_5}{\varphi\ {}^{p}_{5}} + \frac{\varphi_6}{\varphi\ {}^{p}_{6}} \tag{28}$$

where $\varphi_1, \varphi_2, \varphi_3, \varphi_4, \varphi_5$ and φ_6 are the Root of Mean Square (RMS) of the roll angle of the car, roll angle of the trailer, yaw rate of the car, yaw rate of the trailer, lateral acceleration at the CG of the car and lateral acceleration at the CG of the CT combination with the ATDB controller. $\varphi\ {}^{p}_{1}, \varphi\ {}^{p}_{2}, \varphi\ {}^{p}_{3}, \varphi\ {}^{p}_{4}, \varphi\ {}^{p}_{5}$ and $\varphi\ {}^{p}_{6}$ are the RMS of the CT combination without the ATDB controller, which are the counterparts of $\varphi_1, \varphi_2, \varphi_3, \varphi_4, \varphi_5$ and φ_6 respectively. As shown in Eq. (28), each term of the objective function is normalized by the RMS of the corresponding baseline CT combination.

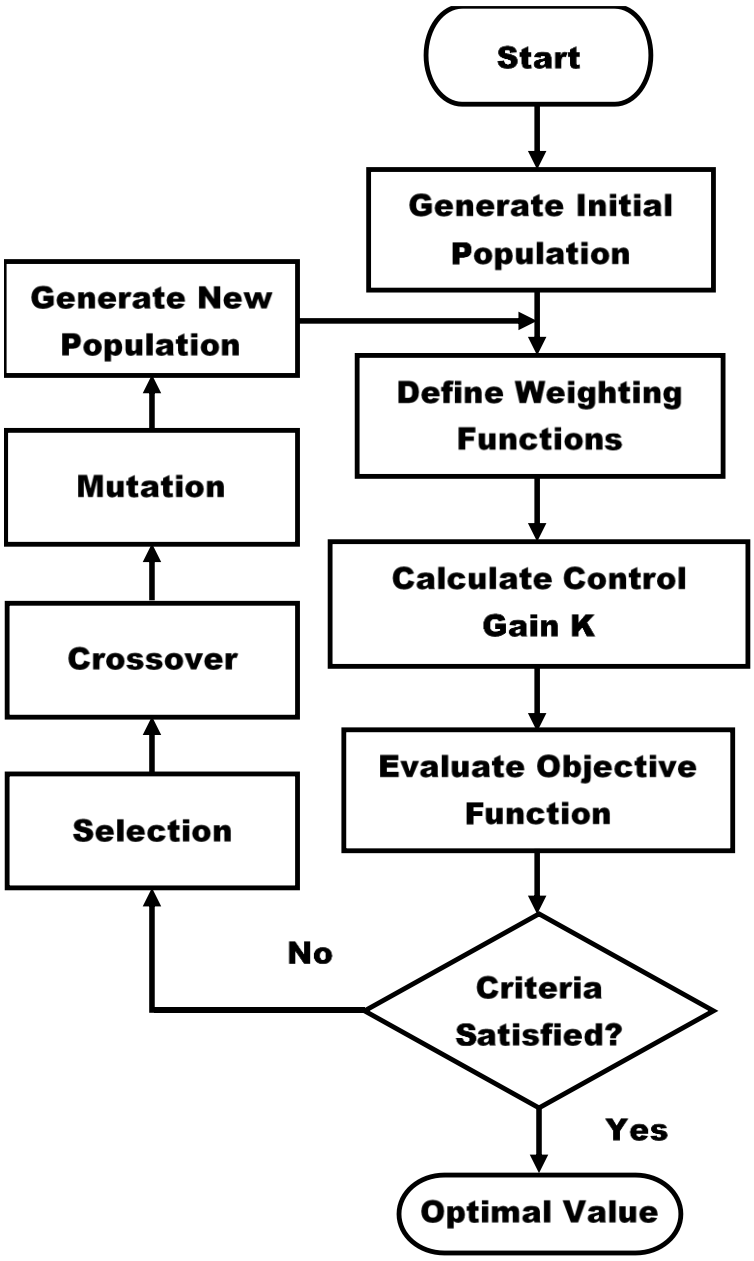

Figure 5-1. GA optimization flow chart

Table 5-1 offers the resulting weighting factors for the low-speed maneuver and high-speed maneuver derived by the GA optimization method.

Table 5-1. The weighting factors determined by the GA

Design Parameters	Low-Speed (60 km/h)	High-Speed (95 km/h)	Bounds
q_1	2.34×10^6	3.7×10^7	$[0,\ 10^8]$
q_2	2.82×10^6	2.79×10^6	$[0,\ 10^8]$
q_3	3.46×10^5	4.28×10^7	$[0,\ 10^8]$
q_4	4.63×10^6	2.13×10^7	$[0,\ 10^8]$
q_5	9.32×10^7	9.95×10^7	$[0,\ 10^8]$
q_6	6.19×10^6	8.63×10^5	$[0,\ 10^8]$
q_7	6.48×10^7	5.49×10^7	$[0,\ 10^8]$
q_8	4.79×10^5	1.96×10^5	$[0,\ 10^8]$
r	0.036	0.0097	[0, 2]

5.3.3 Numerical Simulation

Based on the validated linear 5-DOF model, the ATDB controller is developed and applied for CT combinations. In order to compare the dynamic responses of the CT combination with and without the LQR-based ATDB controller, numerical simulations are conducted under the car front wheel steering angle input of a single cycle of sine-wave with an amplitude of 0.0175 rad and a frequency of 0.318 Hz as shown in Figure 3-2.

5.3.3.1 Numerical Simulation under Low-Speed Maneuver

Figures 5-2 to 5-7 show the dynamic responses of the linear CT model with and without the LQR-based ATDB controller under the single lane-change maneuver at the vehicle forward speed of 60 km/h (a low-speed single lane-change maneuver). A close observation of the simulation results illustrated in Figures 5-2 to 5-7 indicates that the CT combination with the LQR-based ATDB controller outperforms the baseline design in terms of: (1) lateral acceleration at the CG of car, (2) lateral acceleration at the CG of trailer, (3) yaw rate of the car, (4) yaw rate of the trailer, (5) roll angle of the sprung mass of the car, and (6) roll angle of the sprung mass of the trailer.

Figures 5-2 and 5-3 illustrate the time history of the lateral acceleration at the CG of the car and the trailer for the baseline and ATDB controller, respectively. In the case of the linear 5-DOF model with the ATDB controller, the maximum peak value of the lateral acceleration at the CG of the car and trailer is 0.1g and 0.14g, reducing by 38% and 27.3% from the baseline value of 0.17g and 0.19g, respectively.

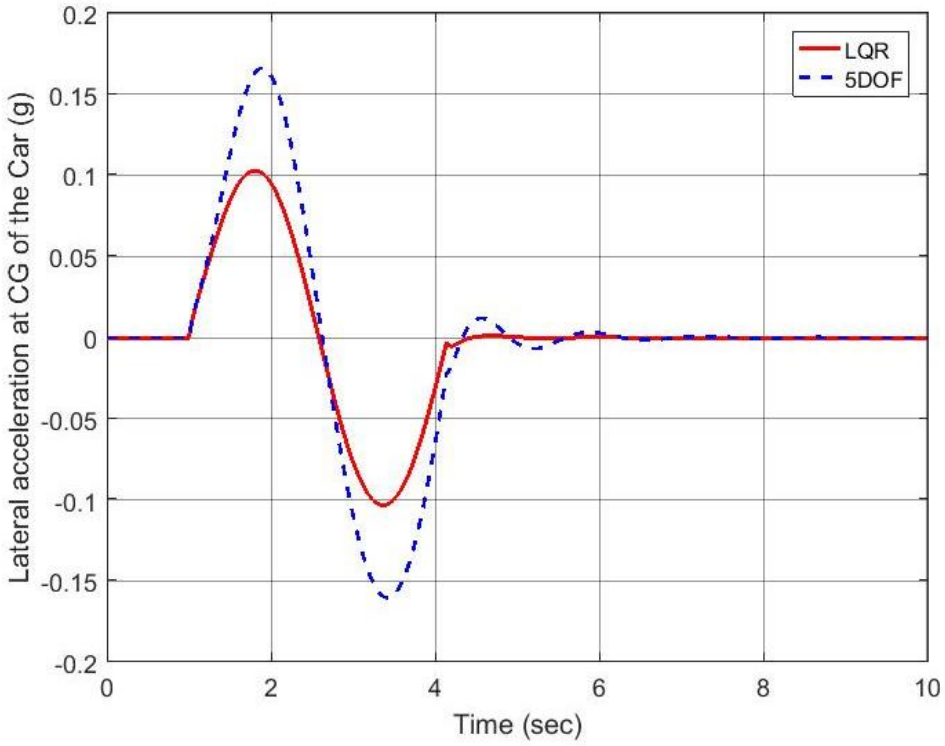

Figure 5-2. Time history of lateral acceleration at the CG of the car (U=60 km/h)

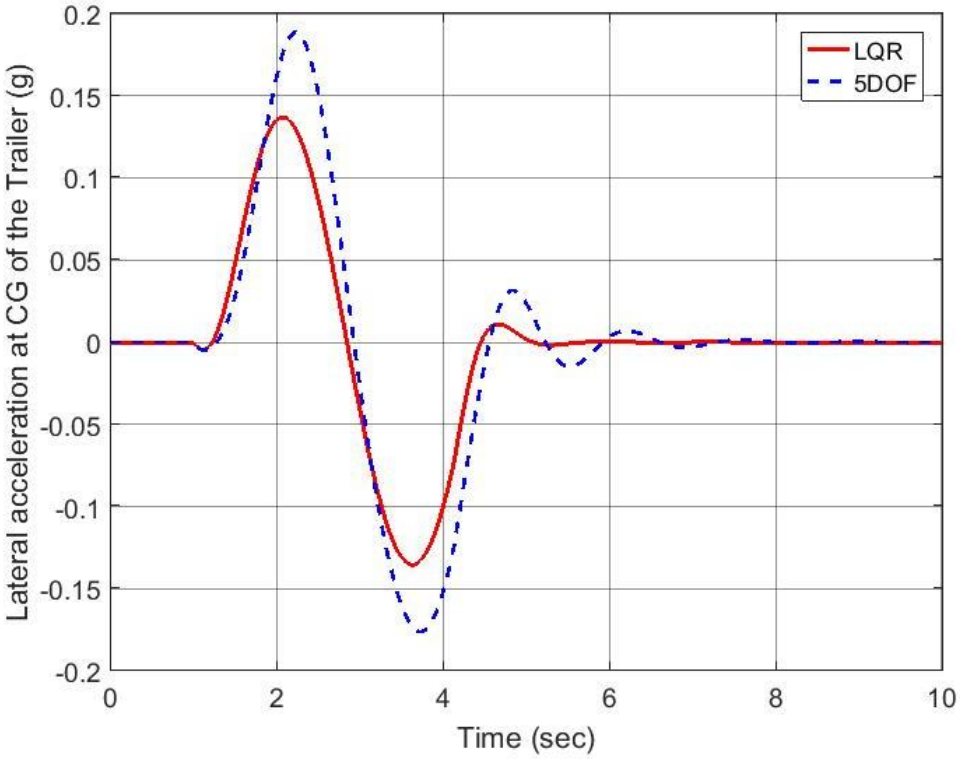

Figure 5-3. Time history of lateral acceleration at the CG of the trailer (U=60 km/h)

Figures 5-4 and 5-5 show that the time history of the car and trailer yaw rate of the linear 5-DOF model for the designs with and without the ATDB controller, respectively. The maximum peak value of the yaw rate of the car and trailer with the ATDB controller are 3.7 deg/s and 4.5 deg/s, reducing by 36.3% and 40.5% from the baseline value of 5.8 deg/s and 7.6 deg/s, respectively.

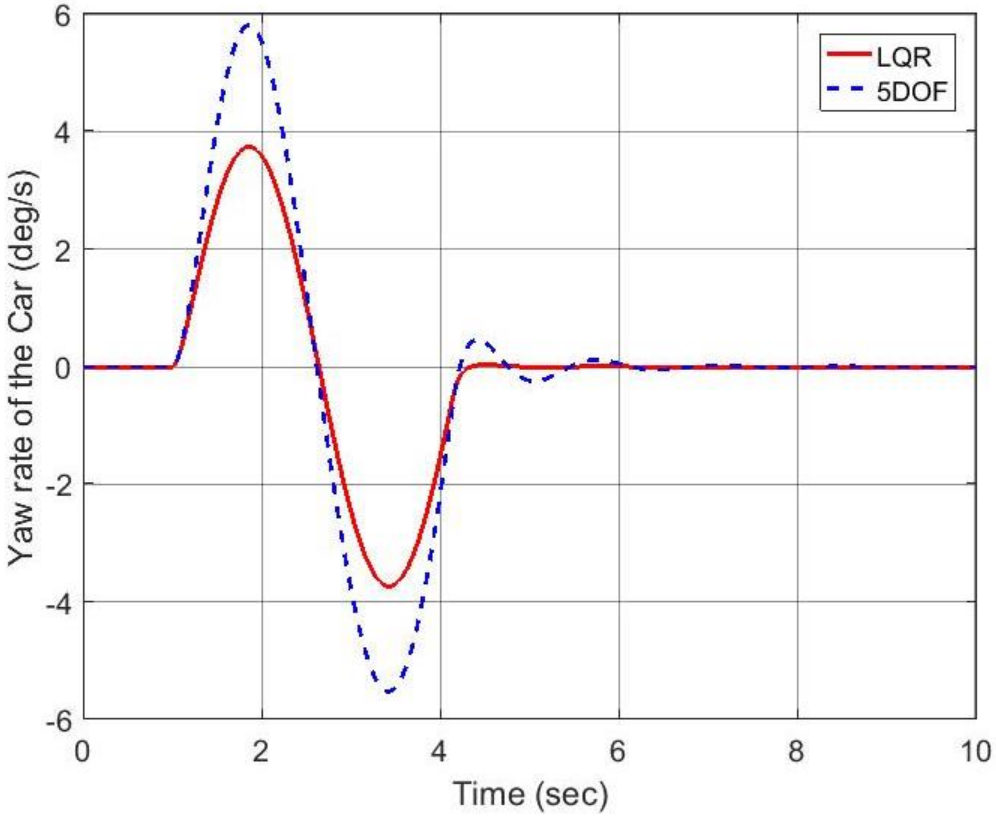

Figure 5-4. Time history of yaw rate of the car (U=60 km/h)

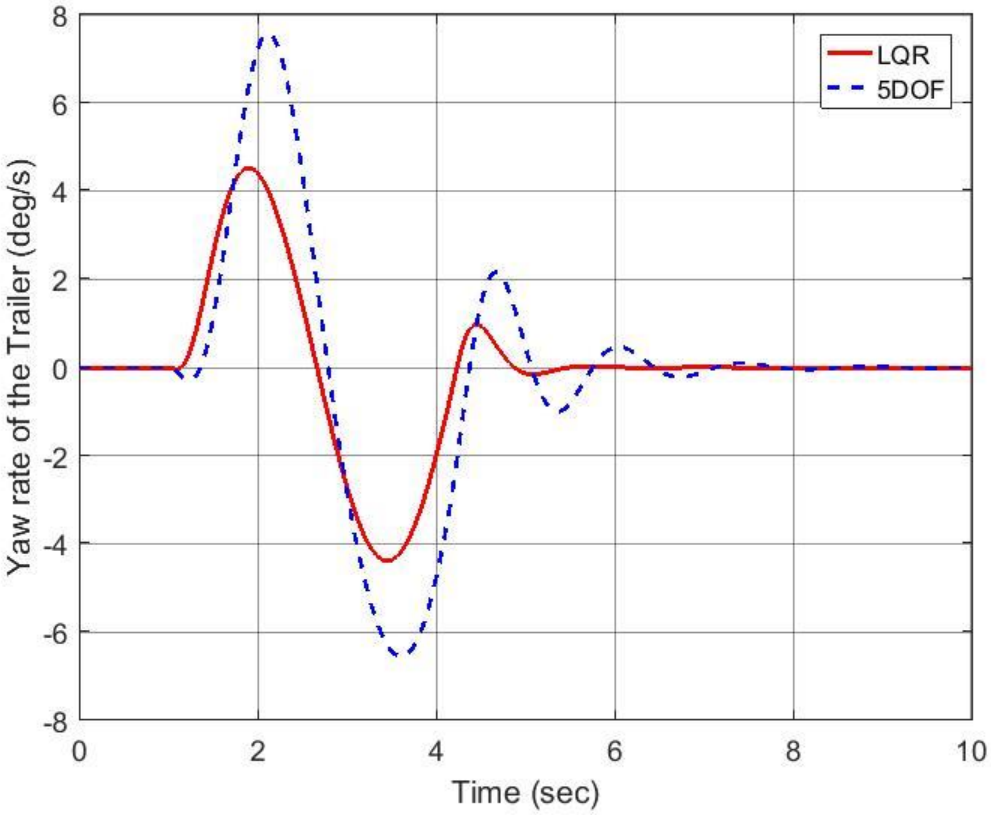

Figure 5-5. Time history of yaw rate of the trailer (U=60 km/h)

Figures 5-6 and 5-7 show the roll angle response of the sprung mass of the car and trailer for the baseline design and the one with the ATDB controller. In the case of the linear 5-DOF model with the ATDB controller, the maximum peak value of the car and trailer roll angle are 0.21 deg and 0.12 deg, reducing by 44.3% and 20.1% from the baseline values of 0.38 deg and 0.15 deg, respectively.

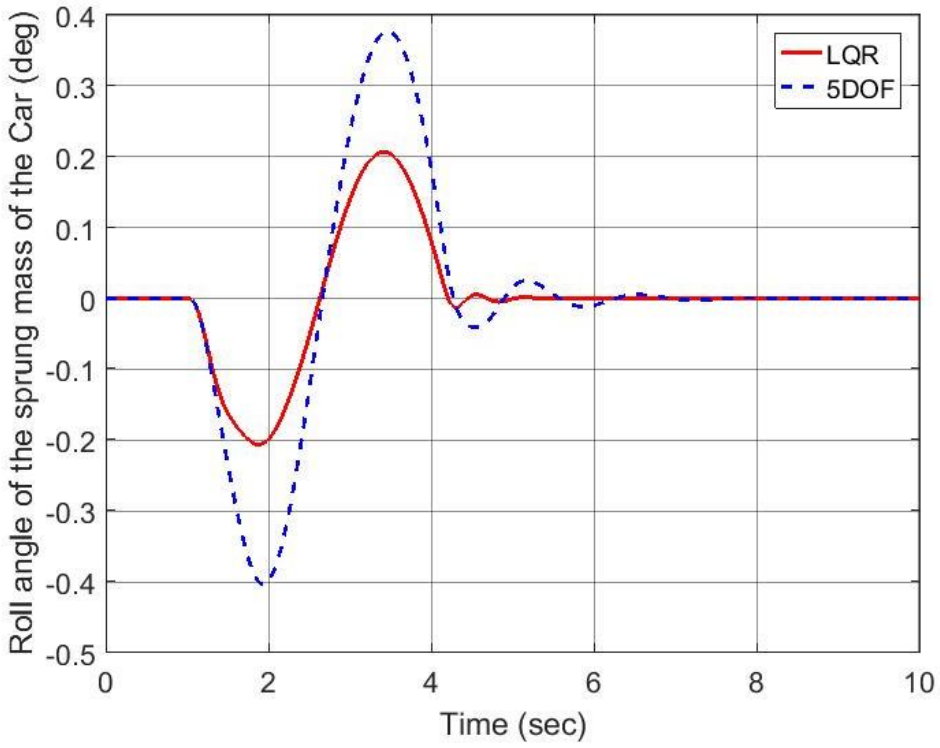

Figure 5-6. Time history of roll angle of the sprung mass of the car (U=60 km/h)

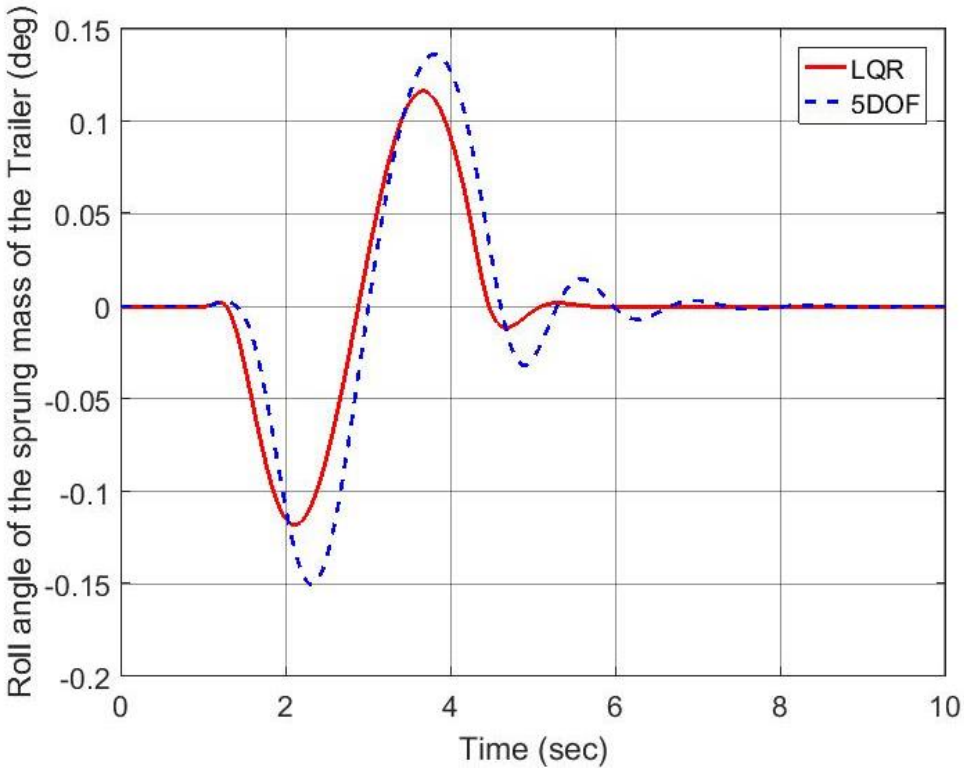

Figure 5-7. Time history of roll angle of the sprung mass of the trailer (U=60 km/h)

5.3.3.2 Numerical Simulation under High-Speed Maneuver

Figures 5-8 to 5-13 show the dynamic responses of the linear CT model with and without the LQR-based ATDB controller under the single lane-change maneuver at the vehicle forward speed of 95 km/h (a high-speed maneuver).

Figures 5-8 and 5-9 illustrate the time history of the lateral acceleration at the CG of the car and the trailer for the baseline and ATDB controller, respectively. The maximum peak value of the lateral acceleration at the CG of the car and trailer with ATDB controller are 0.13g and 0.21g, reducing by 64.7% and 54.9% from the baseline values of 0.37g and 0.46g, respectively.

Figures 5-10 and 5-11 show that the time history of the car and trailer yaw rate of the linear 5-DOF model of the CT combination with and without the ATDB controller, respectively. The maximum peak value of the yaw rate of the car and trailer with ATDB controller are 3.0 deg/s and 5.5 deg/s, reducing by 64.8% and 58.3% from the baseline values of 8.6 deg/s and 13.2 deg/s, respectively.

Figures 5-12 and 5-13 show the simulated roll angle response of the sprung mass of the car and trailer for the CT combination with and without the ATDB controller. In the case of the linear 5-DOF model with ATDB controller, the maximum peak value of the car and trailer roll angle are 0.23 deg and 0.19 deg, reducing by 73.7% and 48.9% from the baseline values of 0.89 deg and 0.37 deg, respectively.

Compared with the baseline case, the oscillation of lateral, yaw and roll motions of the control case is significantly reduced and the settling time is shorter.

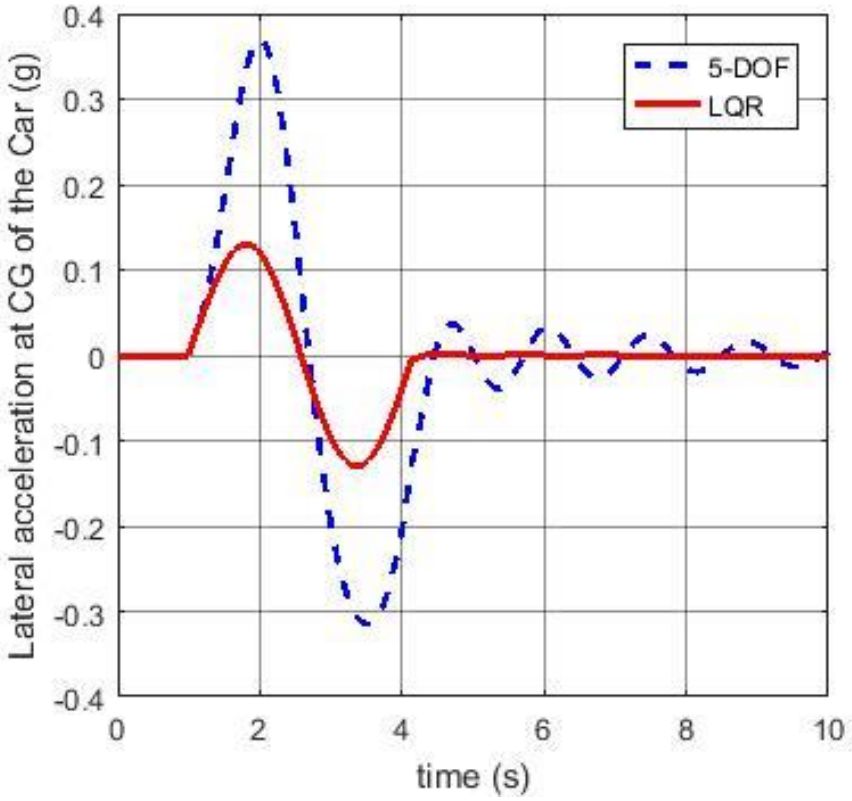

Figure 5-8. Time history of lateral acceleration at the CG of the car (U=95 km/h)

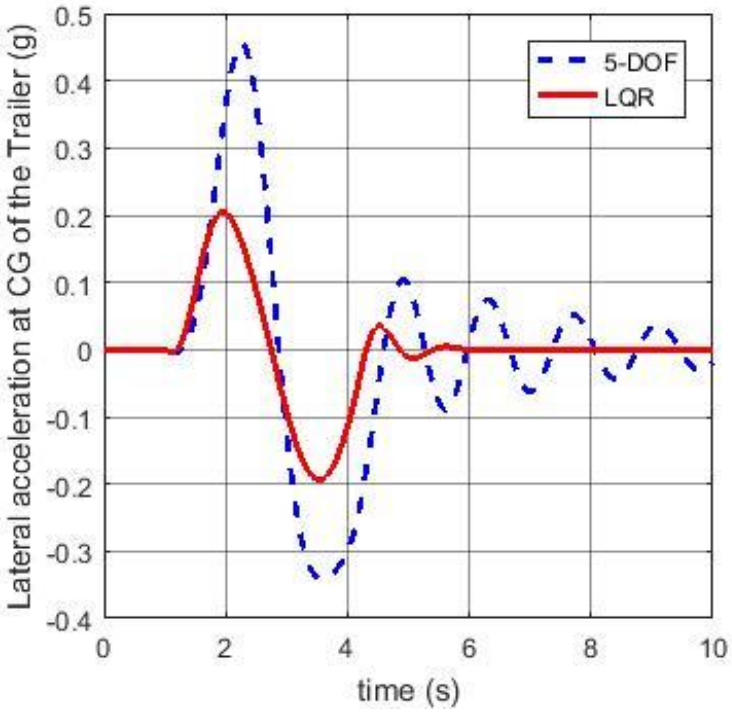

Figure 5-9. Time history of lateral acceleration at the CG of the trailer (U=95 km/h)

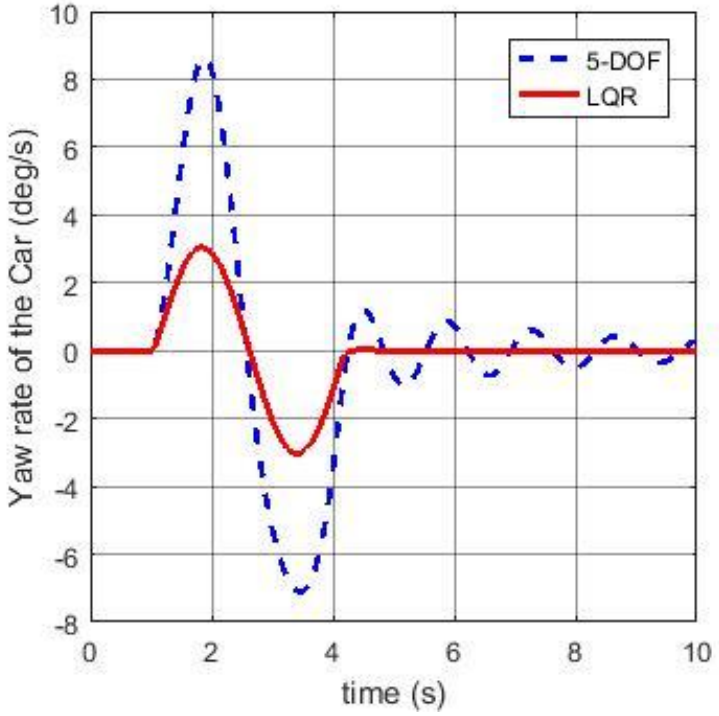

Figure 5-10. Time history of yaw rate of the car (U=95 km/h)

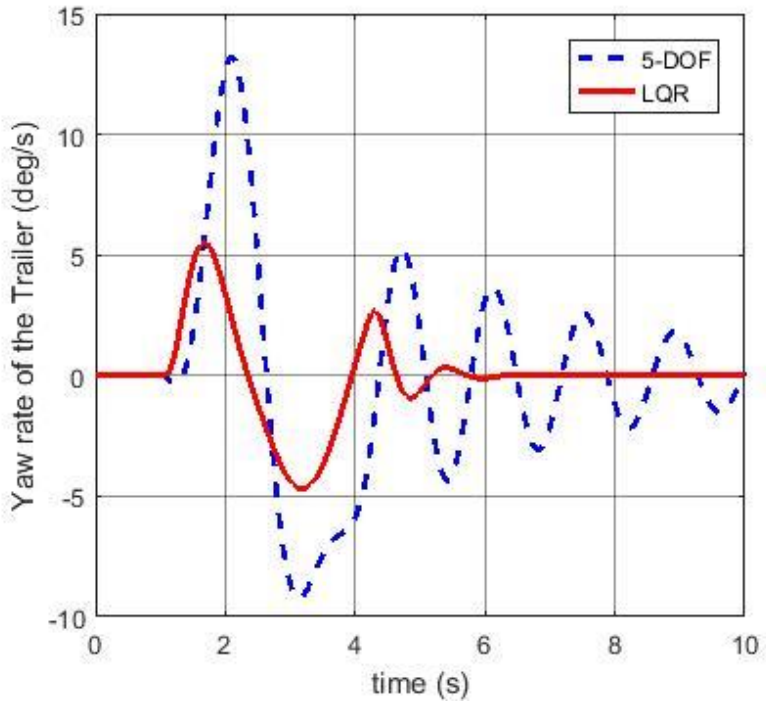

Figure 5-11. Time history of yaw rate of the trailer (U=95 km/h)

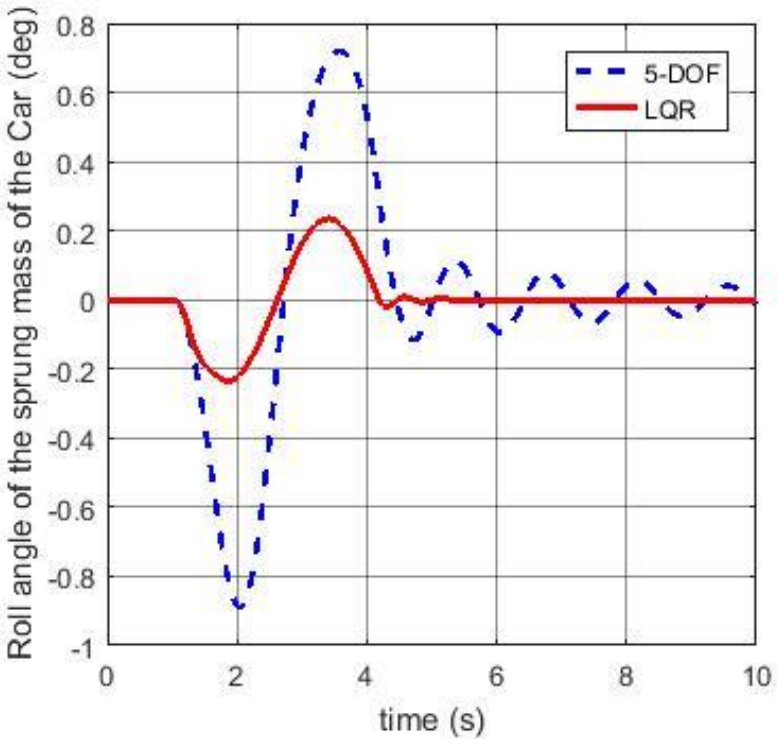

Figure 5-12. Time history of roll angle of the sprung mass of the car (U=95 km/h)

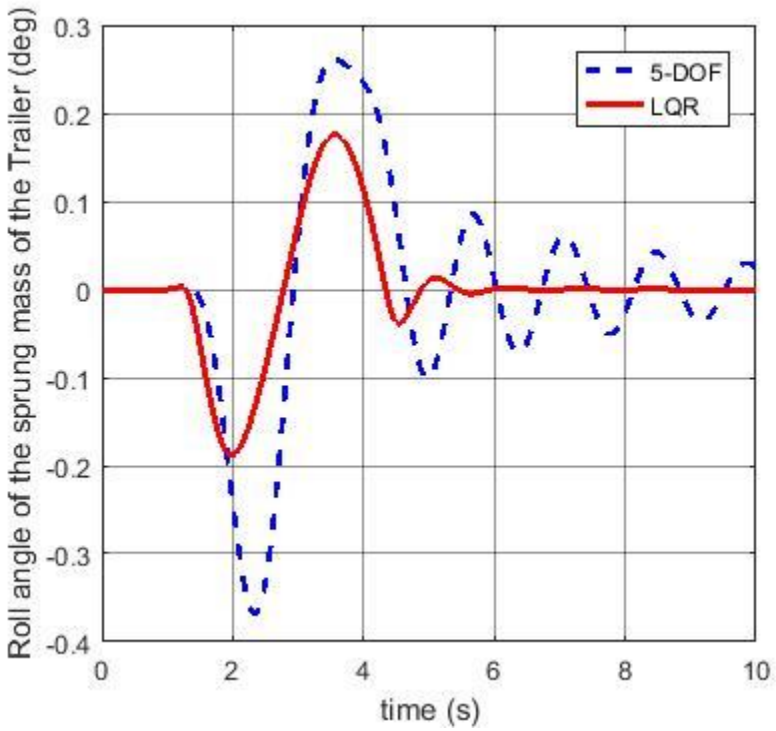

Figure 5-13. Time history of roll angle of the sprung mass of the trailer (U=95 km/h)

5.3.4 Stability Analysis with the LQR-based Controller

In order to further compare the cases with and without the LQR-based ATDB controller, an eigenvalue analysis based on the linear CT model with the ATDB controller is conducted. Note that for this eigenvalue analysis, all vehicle system parameters take their nominal values listed in Appendix A and weighting factors of the low-speed maneuver are used for the ATDB controller. Figure 5-14 shows the damping ratio curves of the 4 least damped motion modes for the case with the ATDB controller. Table 5-2 lists the critical speeds for the cases with and without the ATDB controller. The eigenvalue analysis result shown in Figure 5-14 and Table 5-2 is

consistent with those illustrated in Figures 5-2 to 5-13, which demonstrate that the LQR-based ATDB controller can effectively improve the stability of the CT combination.

Table 5-2. Critical speeds of the CT combination with and without the LQR-based ATDB controller

	Baseline	ATDB controller
Critical Speed (m/s)	31.7	Over 50

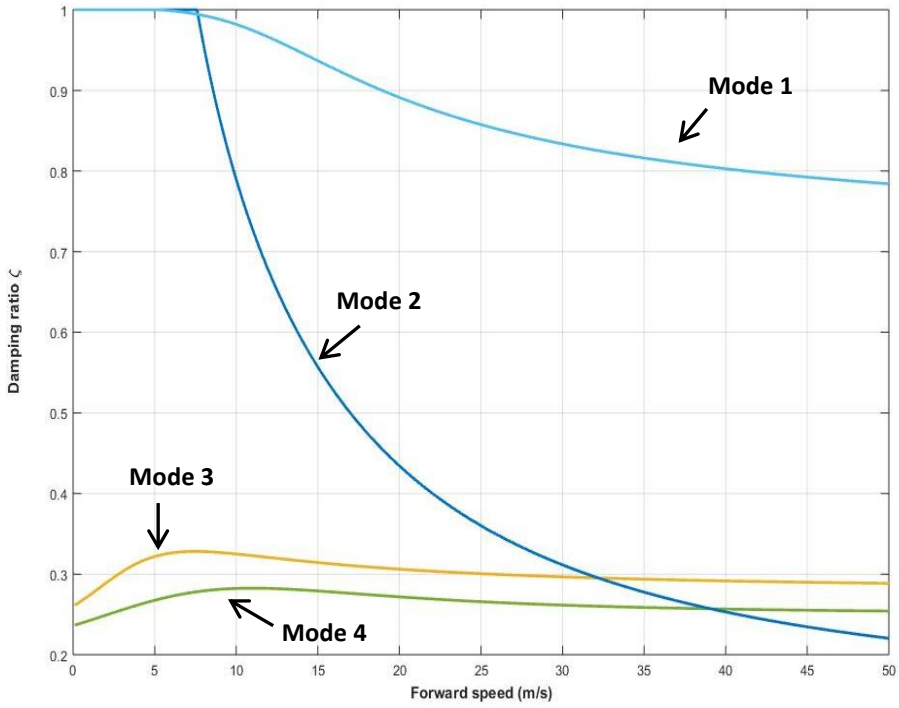

Figure 5-14. Mode damping ratios versus forward speed for the case with the ATDB controller

5.3.5 Summary

An active trailer differential braking (ATDB) controller is designed based on the linear 5-DOF model for the CT combination using the LQR technique. Simulation results demonstrate that with the given nominal values of the vehicle system parameters, the LQR-based ATDB controller can effectively improve the stability of the CT combination under the single lane-change maneuver at the vehicle forward speed of 60 km/h and 95 km/h.

5.4 Robust Controller

5.4.1 Introduction

In previous chapter, the LQR-based ATDB controller is evaluated under a single lane-change maneuver. The simulation results show that the LQR controller exhibits superior performance in improving the stability of CT combinations. From the design point of view, the LQR controller can be designed following a systematic procedure. However, the superior performance of the LQR controller may not be guaranteed in the presence of vehicle model parameter uncertainties, unmodeled dynamics and external disturbances. To address the robust issue of the LQR controller, the H_∞ robust controller, i.e. the μ synthesis controller, is proposed. The μ synthesis controller may ensure robust performance in enhancing the stability of CT

combinations.

Almost all the μ synthesis controllers reported in the literature are designed for single unit vehicles. Little effort has been paid to the design of μ synthesis controllers for articulated vehicle. One of the critical problems in the design of μ synthesis controllers is the selection of weighting functions. Weighting functions impose significant effects on the performance and robustness of μ synthesis controllers. In general, the parameters of weighting functions are chosen using the trial and error method [52]. But, this method is tedious and time-consuming.

In the following sections of this chapter, an ATDB controller is designed using the μ synthesis technique; the μ synthesis controller is derived based on the linear 3-DOF CT model; the weighting function of the robust controller is determined using the GA. To assess the performance of the robust controller, numerical simulations of the CT model with and without the controller are carried out under a single lane-change maneuver.

5.4.2 μ Synthesis Control

In reality, physical vehicle system parameters may not be known accurately or these parameters could be difficult to measure. For example, the mass and yaw moment of inertia of the car and trailer vary with the number of passengers and payloads. In order to control the dynamic behaviors of a CT combination effectively, desired

controllers should be robust to all uncertainties. In this thesis, a total of 7 parameters, i.e. mass of the car and trailer, yaw moment of inertia of the car and trailer and cornering stiffness coefficient of tires, are considered as parametric uncertainties in the design of the robust controller. All values of these parameters can vary by $\pm 30\%$ from their nominal values. Furthermore, the lateral dynamics of a CT combination varies with the change of vehicle forward speed. Some controllers are not guaranteed to be stable at different vehicle forward speeds. To address this problem, the ATDB controller using μ synthesis approach is designed using the linear 3-DOF with vehicle forward speed varying in the range of 40 km/h to 110 km/h. The nominal values and variation of the vehicle system parameters are given in Appendix C.

The μ synthesis is one of the most effective techniques for the robust control design. The main purpose of the robust control is to find a stabilizing controller that ensures the robust stability and performance of the closed-loop system with model parameter uncertainties. The general configuration of the μ synthesis control scheme is shown in Figure 5-15. In Figure 5-15, d denotes the external inputs; e denotes the output errors; y_{un} and $Pert$ are the input and output signals of the dynamic uncertainties; y and u represent the feedback signals and the control signal, respectively; P is the nominal plant model with the weighting functions; Δ is the plant perturbations.

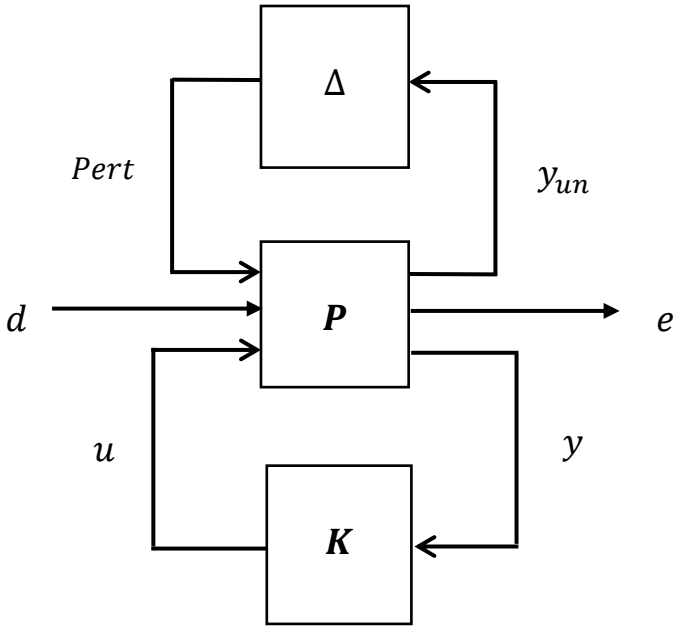

Figure 5-15. General configuration of μ synthesis

For the controller design, it is required to find a control gain K, which stabilizes the closed-loop system and satisfies Eq. (29) for all uncertainties [47].

$$\|F_u[F_l(P,K),\Delta]\|_\infty < 1 \tag{29}$$

For the robust performance of the system, the augmented uncertainty structure Δ_P is defined as

$$\Delta_P := \begin{bmatrix} \Delta & 0 \\ 0 & \Delta_F \end{bmatrix} \tag{30}$$

where Δ is parametric uncertainty block and Δ_F is the fictitious complex uncertain block. The robust performance analysis of the system can be done by using the structured singular value of $F_l(P,K)(j\omega)$ in respect of the extended uncertainty Δ_P. The goal of μ synthesis is to minimize the peak value of the singular value $\mu_{\Delta_P}(\cdot)$ of

the corresponding closed-loop transfer function for all uncertainties over all stabilizing controllers as shown in Eq. (31) [43, 46].

$$\min_{\substack{K \\ stabilizing}} \max_{\omega} \mu_{\Delta_P}[F_l(P,K)(j\omega)] \tag{31}$$

To achieve the stability and performance robustness of the system, the structured singular value μ_{Δ_P} is required to satisfy the following condition.

$$\mu_{\Delta_P}[F_l(P,K)(j\omega)] < 1 \tag{32}$$

5.4.3 Controller Design and Optimization

Finding suitable weighting functions is an important step in robust controller design and normally need a few trials. Usually, the weighting functions are selected from proper, minimum phase transfer functions of low or high pass filters, based on their purpose of application. In this thesis, five weighting functions are considered. The block diagram of the closed-loop CT combination with weighting functions is shown in Figure 5-16.

The weighting function matrix $\mathbf{W}_n$ serves to model sensor noises n_1 and n_2 at the measurements of yaw rate of the car and trailer, respectively. The control input u is weighted beyond according to the input limitation by the weighting function W_u. The weighting function matrix $\mathbf{W}_\mathrm{p}$ is applied on the performance outputs, which are

related with the yaw rates of the car and trailer, respectively. The weighting functions of the closed-loop CT system can be described by the following formulas [51]:

$$\mathbf{W_p} = diag\left[\frac{{}^{s}/_{M_1} + \omega_1}{s + \omega_1\epsilon_1}, \frac{{}^{s}/_{M_2} + \omega_2}{s + \omega_2\epsilon_2}\right] \tag{33}$$

$$W_u = \frac{s + \omega_3/M_3}{\epsilon_3 s + \omega_3} \tag{34}$$

$$\mathbf{W_n} = diag\left[\frac{s + {}^{\omega_4}/_{M_4}}{\epsilon_4 s + \omega_4}, \frac{s + {}^{\omega_5}/_{M_5}}{\epsilon_5 s + \omega_5}\right] \tag{35}$$

where the steady sate error is not greater than ϵ_i, ω_i is the crossover bandwidth and M_i is the sensitivity peak ($i = 1, 2, 3, 4\ and\ 5$).

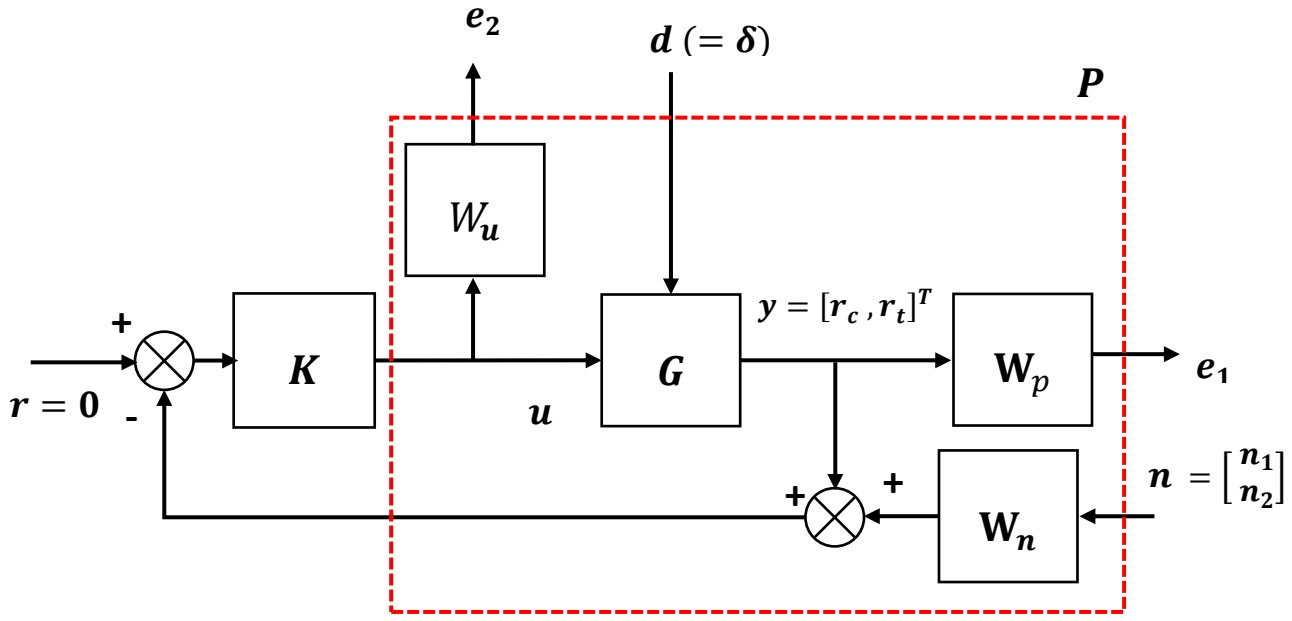

Figure 5-16. The block diagram of the closed-loop CT system

For a robust control design, it is required to select optimal weighting function parameters to satisfy the robust stability and performance of the system. However, even though many researches have been reported about μ synthesis control, the parameters of weighting functions are tuned by the conventional trial and error method. This approach is difficult to use without knowledge of the frequency domain response. In order to design optimal robust controller, the GA is introduced in this section. The design optimization is to find optimal values of the design variables in order to minimize the objective function.

In order to achieve closed-loop robust performance, it is desired to satisfy following performance objective function.

$$J_{cost} = \left\| \begin{bmatrix} W_p S_o G & -W_p S_o G K W_n \\ -W_u K S_o G & -W_u K S_o W_n \end{bmatrix} \right\|_\infty < 1 \tag{36}$$

where

$$S_o = (I + GK)^{-1} \tag{37}$$

is the output sensitivity function and K is the optimal control gain matrix by using *dksyn()* function in MATLAB. The objective function is defined as shown Eq. (36), it can be evaluated using the optimization toolbox in MATLAB.

5.4.4 Simulation Results

The robust ATDB controller for the CT system is designed in MATLAB and the performance of the ATDB controller is evaluated under the single-lane change

maneuver as shown in Figure 3-2. The weighting parameters of the μ synthesis controller are obtained using the GA, which are listed in Table 5-3.

In order to examine the effectiveness of the proposed robust ATDB controller, the transient responses of the nominal system with and without the controller are compared. Figures 5-17 and 5-18 show the dynamic responses of the nominal CT model with and without the μ synthesis based ATDB controller under the single lane-change maneuver. It is clear that the CT system with the μ synthesis controller exhibits a better performance than that of the CT system without the controller. In the case of the nominal 3-DOF model with the robust controller, the maximum peak values of the yaw rate of the car and trailer are decreased by 46.9% and 58.3% from the baseline values of 5.8 deg/s and 7.5 deg/s to the controlled values of 3.08 deg/s and 3.13 deg/s. Also the maximum peak values of the lateral acceleration at the CG of the car and trailer with the robust controller are 0.087g and 0.096g, reducing by 47.3% and 48.5% from the baseline values of 0.17g and 0.19g, respectively. It is observed that for the robust ATDB controller, the settling time is decreased and oscillation is reduced compared with the CT system without the robust ATDB controller.

Table 5-3. Weighting parameters of μ synthesis controller determined by the GA

Weighting Functions	Parameters
$\mathbf{W_p}$	$diag\left[\frac{1.468\,s+1.742}{s+2.689*10^6}, \frac{0.7495\,s+2.209}{s+18086}\right]$
W_u	$\frac{3.02*10^{-2}s\ +1}{s+10^8}$
$\mathbf{W_n}$	$diag\left[\frac{0.00229\,s\ +0.1}{0.2838\,s+1}, \frac{0.03433\,s\ +0.1}{10^{-8}\,s+1}\right]$

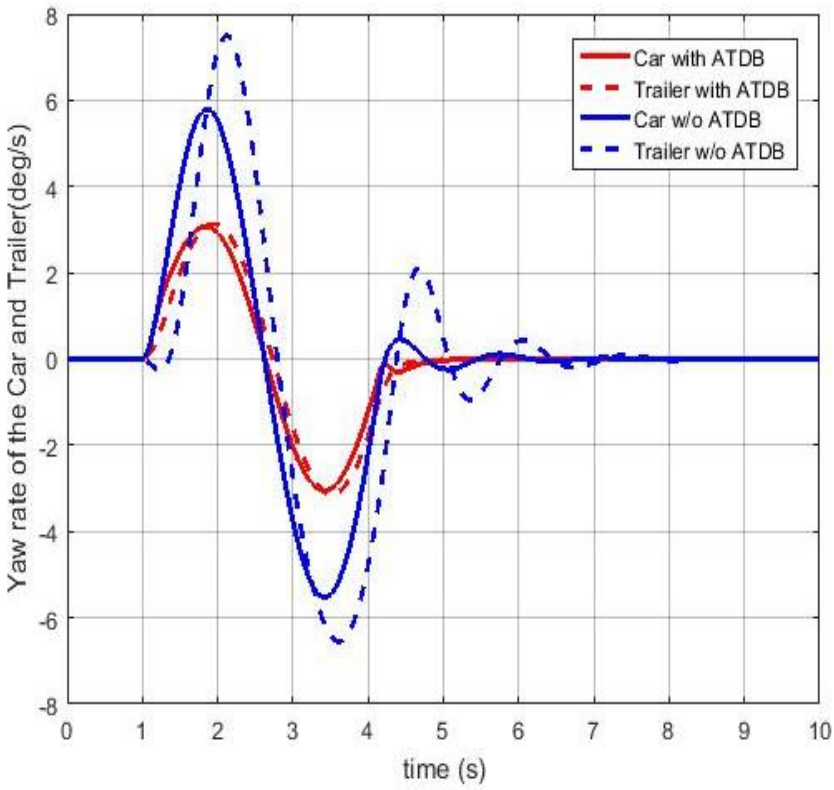

Figure 5-17. Time history of yaw rate of the car and trailer

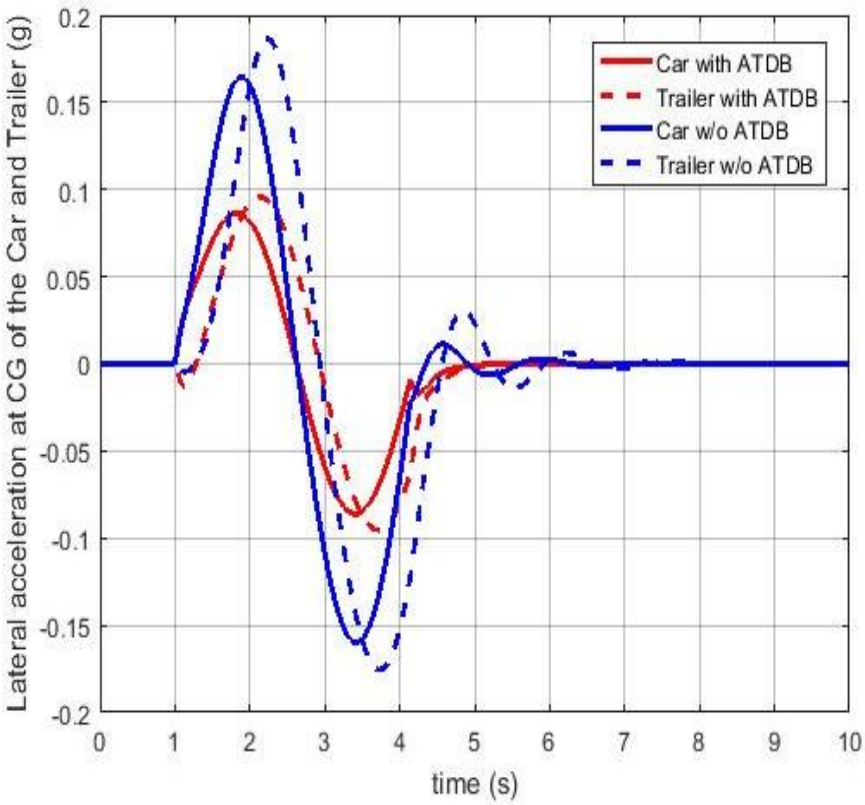

Figure 5-18. Time history of lateral acceleration of the car and trailer

The success of the robust ATDB controller can be assessed in terms of the μ value achieved. The robust performance analysis is conducted to check the robustness of the closed-loop CT combination with model parameter uncertainties as shown in Figure 5-19. As seen in this figure, the peak μ value is 0.976, which is less than 1 and satisfies the robust performance condition expressed in Eq. (32). It is indicated that the closed-loop CT combination achieves the performance robustness to parametric uncertainties.

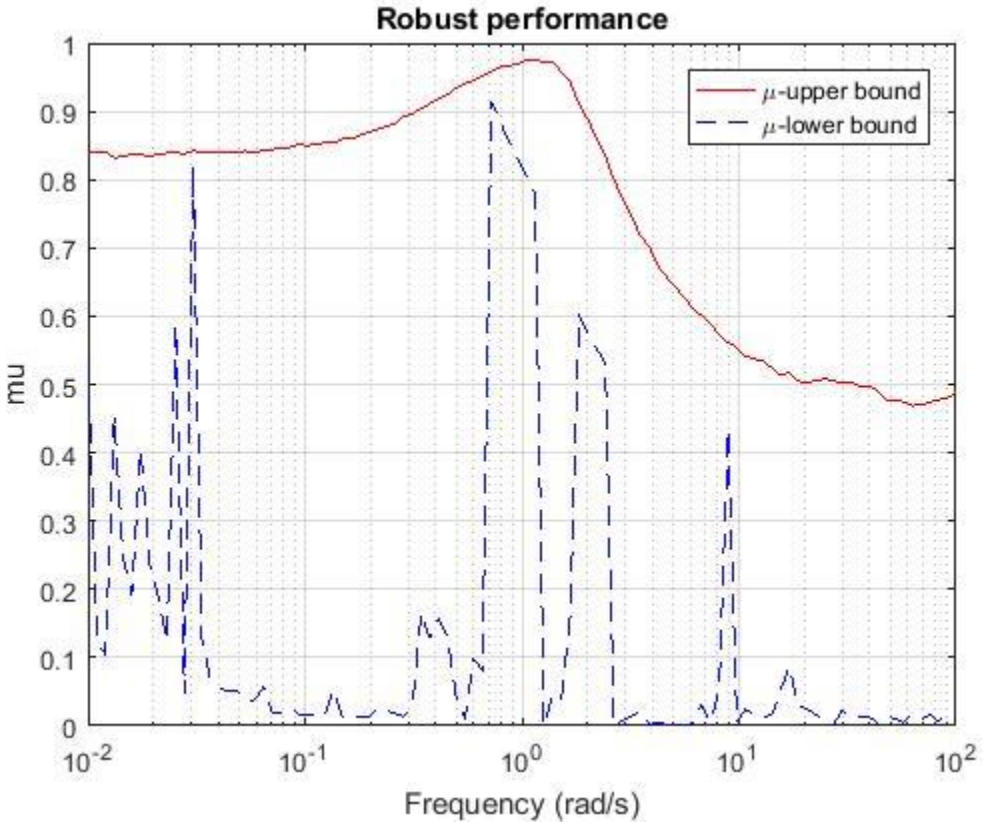

Figure 5-19. μ plot of the robust performance

In order to satisfy the performance criterion shown in Eq. (36), it is necessary that the magnitude responses of the output sensitivity function with system uncertainties lie below the magnitude responses of the inverse of the performance weighting functions in the whole frequency range [43, 51]. Figures 5-20 and 5-21 show that the output sensitivity function lies below the inverse of the performance weighting functions, $\mathbf{W_p}$. W_{p_1} and W_{p_2} are the performance weighting function of the car yaw rate and trailer yaw rate, respectively. It is clear that the performance criterion is satisfied.

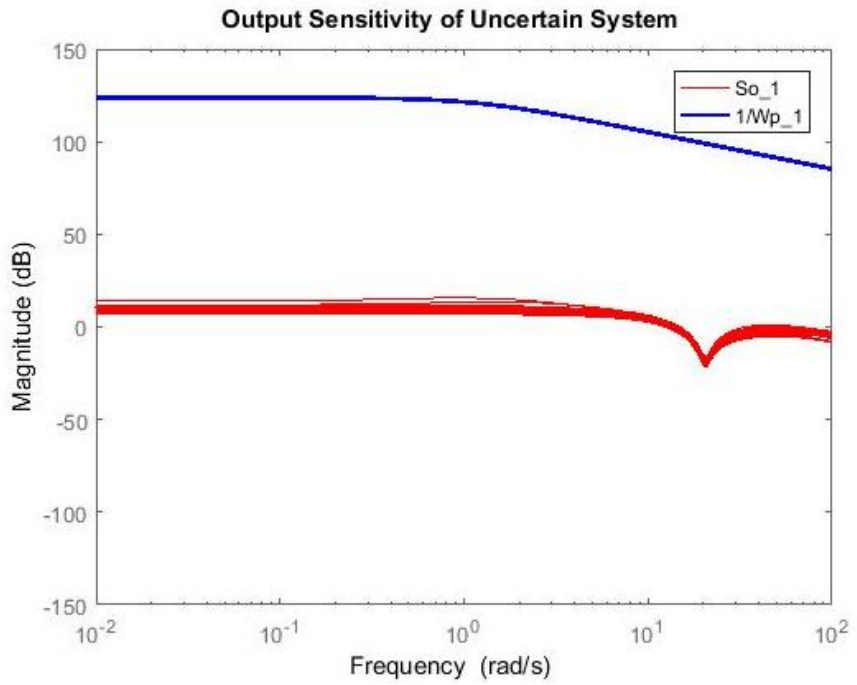

Figure 5-20. Output sensitivity function and inverse of performance weighting functions (W_{p_1})

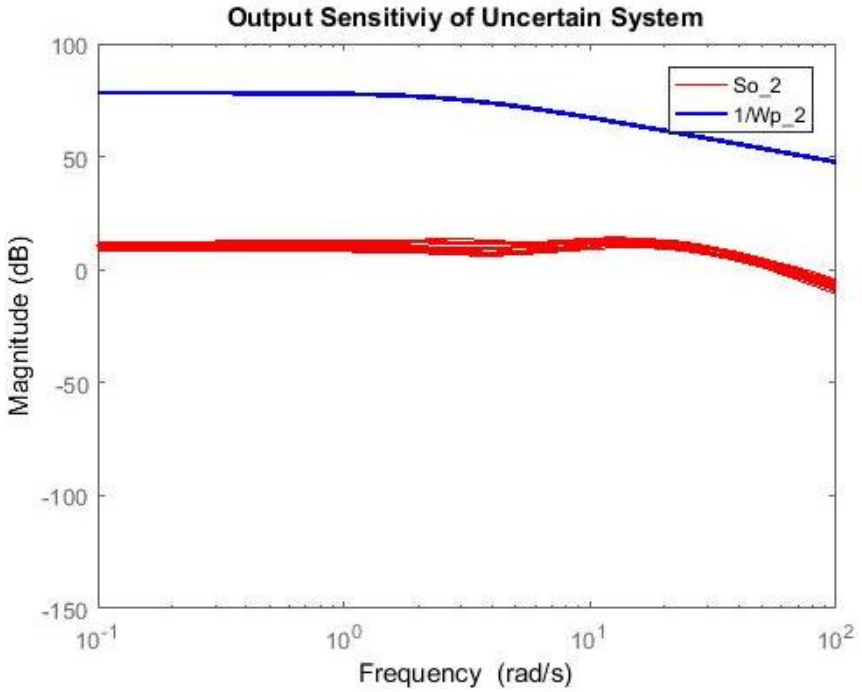

Figure 5-21. Output sensitivity function and inverse of performance weighting function (W_{p_2})

To investigate the effects of the parametric uncertainties on the performance of the CT combination with and without the robust ATDB controller, simulations are performed considering 100 random parameter uncertainties using *usample()* function in MATLAB. This function generates random samples of uncertain model. The robust performance of the μ synthesis controller is demonstrated in terms of the simulation results shown in Figures 5-22 to 5-25, which take into account of 100 random parameter uncertainties.

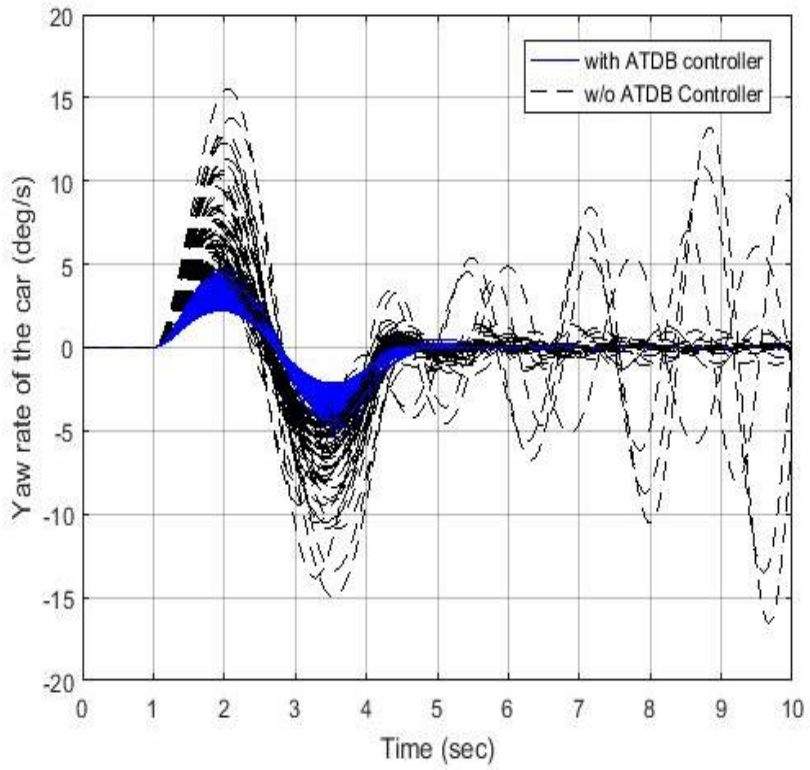

Figure 5-22. Time history of yaw rate of the car with 100 random uncertainties

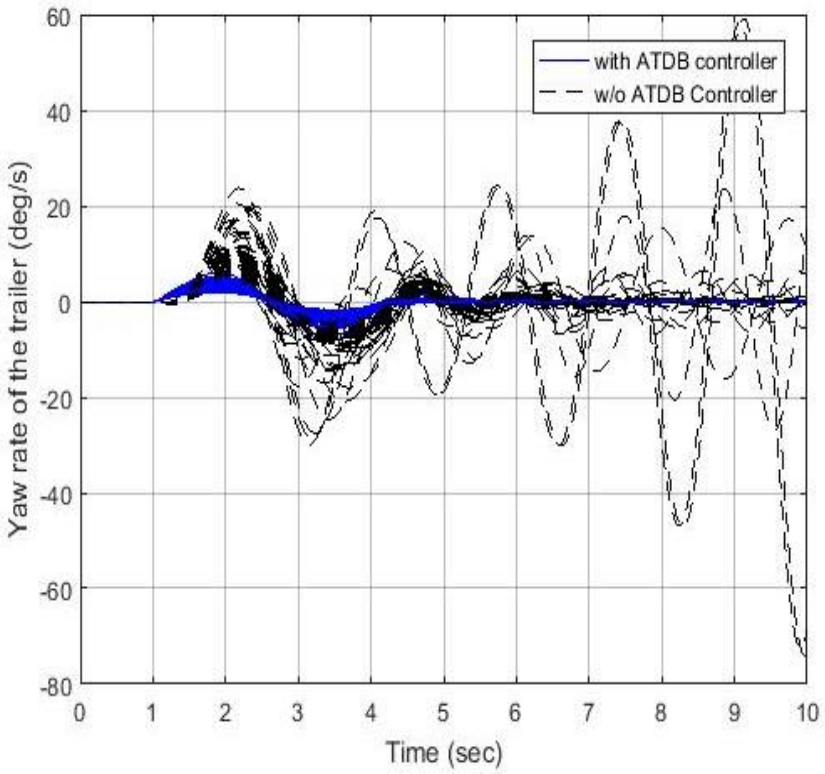

Figure 5-23. Time history of yaw rate of the trailer with 100 random uncertainties

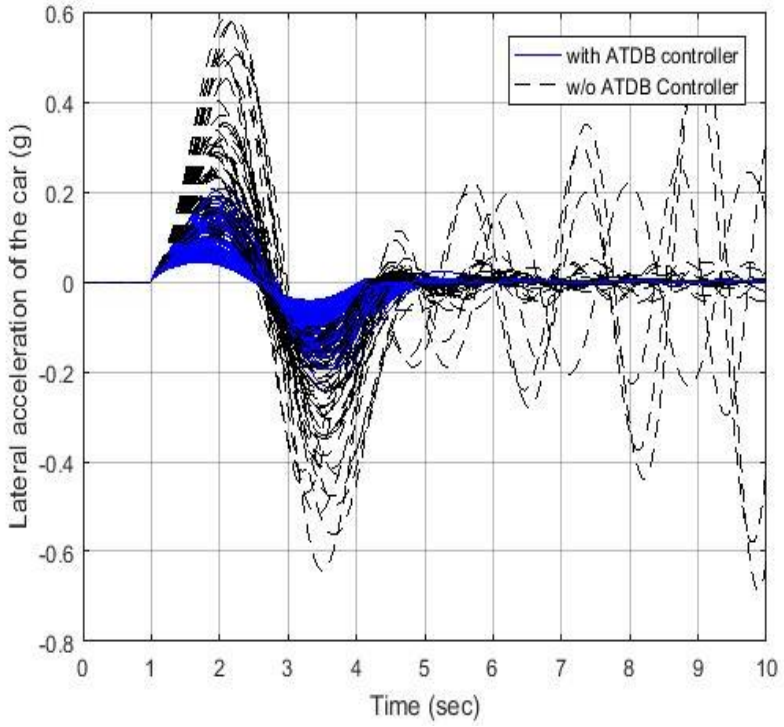

Figure 5-24. Time history of lateral acceleration of the car with 100 random uncertainties

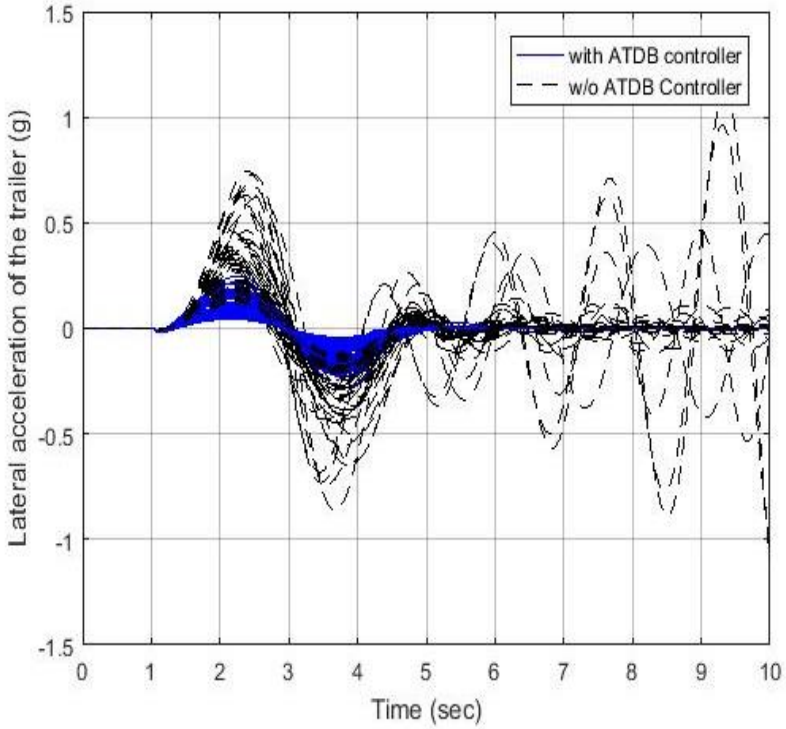

Figure 5-25. Time history of lateral acceleration of the trailer with 100 random uncertainties

In order to examine the robustness of the controller, the worst case is simulated for the CT combination with and without the robust ATDB controller under the single lane-change maneuver. The worst case is the combination of maximum forward speed, minimum yaw moment inertia of the car, maximum yaw moment inertia of the trailer, maximum cornering stiffness of car front tires, minimum cornering stiffness of car rear tires, minimum cornering stiffness of the trailer tires, minimum total mass of the car and maximum total mass of the trailer as listed in Appendix C. As shown in Figures 5-26 to 5-29, the dynamic responses of the CT combination without the robust ATDB controller are unstable, while the dynamic responses of the CT

combination with the robust ATDB controller are stable. The simulation results indicate that the robust ATDB controller is stable over the wide range of parameter uncertainties, and the controller can guarantee robust performance of the CT combination.

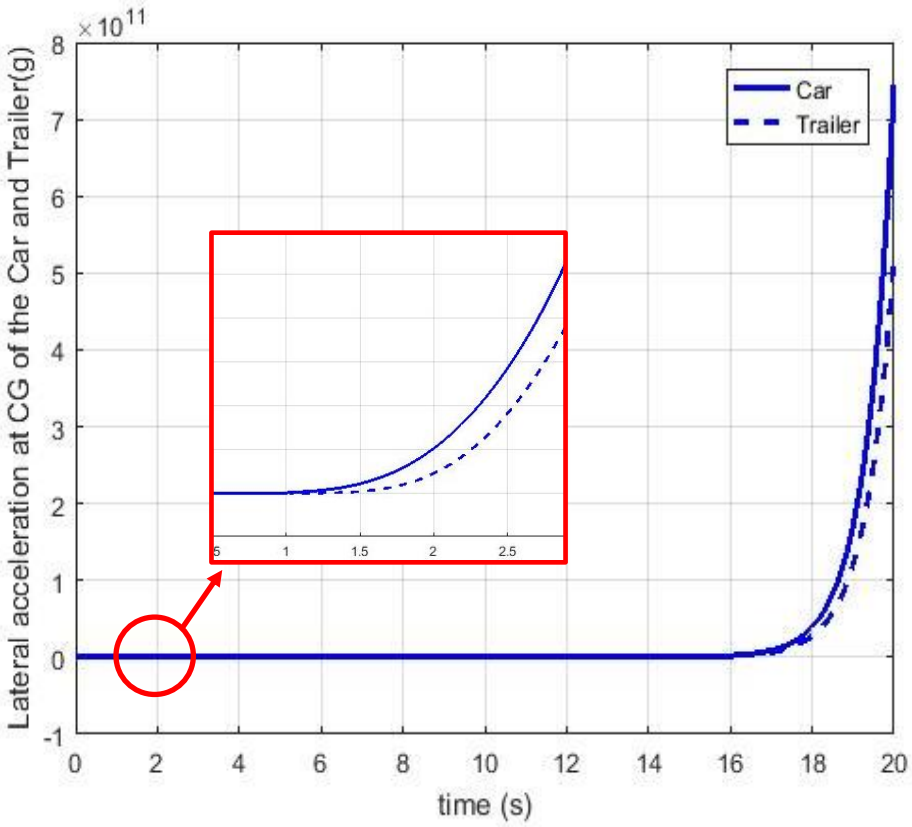

Figure 5-26. Time history of lateral acceleration of the car and trailer with the worst case parameter set for the CT combination without the robust ATDB controller

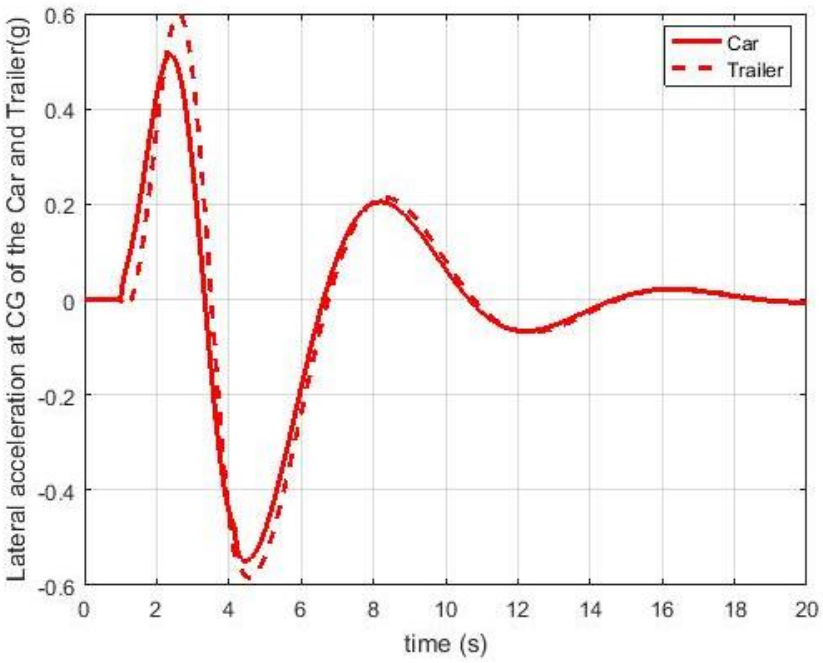

Figure 5-27. Time history of lateral acceleration of the car and trailer with the worst case parameter set for the CT combination with the robust ATDB controller

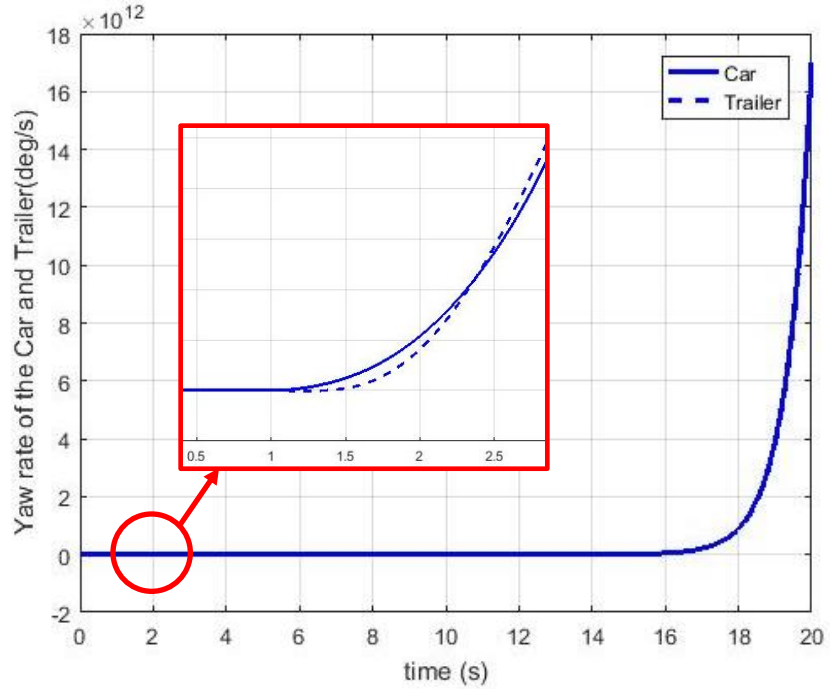

Figure 5-28. Time history of yaw rate of the car and trailer with the worst case parameter set for the CT combination without the robust ATDB controller

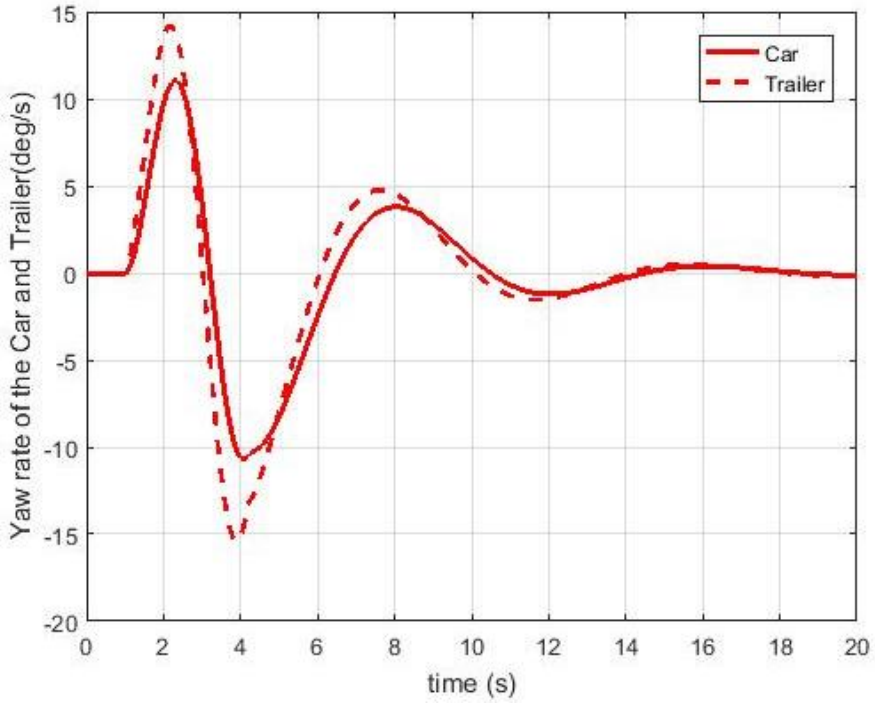

Figure 5-29. Time history of yaw rate of the car and trailer with the worst case parameter set for the CT combination with the robust ATDB controller

5.4.5 Summary

In this section, the μ synthesis based ATDB controller is designed and the robustness of the controller is evaluated using numerical simulation based on the linear 3-DOF CT model. It is observed that the μ synthesis based ATDB controller can effectively enhance the lateral stability of the CT combination considering model parameter uncertainties and sensor noises. Suitable formulations of the weighting functions for the robust controller have been selected, and the weighting functions are optimized using GA by minimizing the objective function. The application of the GA to the robust

controller design can facilitate the design implementation and improve the performance of the controller. Simulation results demonstrate that the proposed robust ATDB controller tuned by the GA can enhance the lateral stability of the CT combination subject to system uncertainties.

6.Conclusions and Recommendations

6.1 Conclusions

This thesis presents the design, validation and optimization of active trailer differential braking (ATDB) systems for car-trailer (CT) combinations. In order to design the controllers for the ATDB systems, a linear yaw-plane model with 3 degrees of freedom (DOF) and a linear yaw-roll model with 5-DOF are generated and validated using a nonlinear model developed in CarSim commercial software package. The linear models and the CarSim model are in good agreement in terms of the lateral accelerations of car and trailer, the yaw rates of car and trailer and roll angles of car and trailer under the low-speed (60 km/h) single lane-change maneuver. There exist some differences between the linear 5-DOF model and CarSim model under the high-speed (95 km/h) single lane-change maneuver due to different tire models used. However, the 5-DOF model can still simulate the dynamic responses of the CT combination, which are similar to those mimicked by the nonlinear CarSim model.

In the case of the linear stability analysis for the CT combination, parametric studies are carried out using eigenvalue analysis based on the linear yaw-roll 5-DOF model. Through the eigenvalue analysis, critical speeds of the CT combination with varying

trailer parameters have been identified. The eigenvalue analysis indicates that decreasing the distance between the trailer CG and the hitch (i.e., increasing the tongue load of the hitch), reducing trailer yaw inertia, increasing the distance between trailer axle and hitch and increasing trailer sprung mass are beneficial for enhancing the stability of the CT combination. The aforementioned observations may be used as qualitative guidelines in CT combination design and trailer applications considering operating conditions and various constraints, such as vehicle safety standards or regulations.

The validated linear 5-DOF model is used to design an ATDB controller using the linear quadratic regulator (LQR) technique. Numerical simulation results show that the CT combination with the LQR-based ATDB controller outperforms the baseline CT combination in terms of all dynamic responses under the single lane-change maneuver at the vehicle forward speeds of 60 km/h and 95 km/h. It clearly indicates that the ATDB controller is a promising solution to the safety enhancement of CT combinations.

The LQR technique has been widely used in design of control systems in recent years. However, the LQR controller may not work well when the system parameters and operating conditions are not known exactly. To explore robustness of ATDB control, the μ synthesis controller is proposed for CT combinations. The robust ATDB controller using μ synthesis approach is designed using the linear 3-DOF

considering varying vehicle forward speed (40 km/h to 110 km/h) and 7 uncertain system parameters. Simulation results indicate that the μ synthesis controller can effectively improve the lateral stability of the CT combination and achieve the robust stability and robust performance subject to parametric uncertainties.

In order to design optimal ATDB controllers, a genetic algorithm (GA) provided in MATLAB optimization toolbox is used in this thesis. The optimization results show that the application of the GA can facilitate the design implementation of the ATDB controllers.

6.2 Recommendations for Future Research

To further examine and improve the proposed ATDB controllers, the following recommendations are made:

1. In order to improve the fidelity of CT models, nonlinear models, such as the CarSim model used in the current research, should be used to design and evaluate controllers.
2. Driver-software-in-the-loop (DSIL) or driver-hardware-in-the-loop (DHIL) real-time simulation may be applied to evaluate controllers' performance.

References

[1] X. Yang, Optimal Reconfiguration Control of the Yaw Stability of the Tractor-Semitrailer Vehicle, *Mathematical Problems in Engineering*, Volume 2012.

[2] BigTex Trailers, http://bigtextrailers.com/single-axle-vs-tandem-axle-whats-the-difference/

[3] A. Clay, J. Montufar, and D. Middleton, Operation of long semi-trailers in the United States, *Transportation Research Record*, Vol.1833, pp.79-86. 2003.

[4] F. Vlk, Handling Performance of Truck-Trailer Vehicles: A State-of-the-Art Survey, *Int. J. Of Vehicle Design* 6(3), pp.323-361. 1985.

[5] A. Hac, D. Fulk, and H. Chen, Stability and Control Consideration of Vehicle-Trailer Combination, *SAE Technical Paper*, Paper No: 2008-01-1228, 2008.

[6] R. Shamim, M. M. Islam, and Y. He, A Comparative Study of Active Control Strategies for Improving Lateral Stability of Car-Trailer Systems, *SAE Technical Paper*, Paper No: 2011-01-0959, 2011.

[7] E.F. Kurtz Jr. and R.J. Anderson, Handling Characteristics of Car-Trailer Systems: A State-of-the-Art Survey, *Vehicle Systems Dynamics*, Vo1.6, pp. 217-243, 1977.

[8] Q. Wang, Design and Validation of Active Trailer Steering Systems for Articulated Heavy Vehicles Using Driver-Hardwar-in-the-Loop Real-Time Simulation, *Master Thesis, University of Ontario Institute of Technology*, 2015.

[9] M. El-Gindy, N. Mrad and X. Tong, Sensitivity of rearward amplification control of a truck/full trailer to tyre cornering stiffness variations, *Proceeding of the IMechE Part D: Journal of Automobile Engineering*, Vol. 215, pp. 579-588, 2001.

[10] P. Liu, Analysis, Detection and Early Warning Control of Dynamic Rollover of Heavy Freight Vehicles, *Concordia University*, 1999.

[11] T. Sun, Design Synthesis of Car-Trailer Systems with Active Trailer Differential Braking Strategies, *Master Thesis, University of Ontario Institute of Technology*, 2013.

[12] J. M. Williams Jr. and F. Mohn, Trailer Stabilization Through Active Braking of the Towing Vehicle, *SAE Technical Paper*, Paper No: 2004-01-1069, 2004.

[13] National Highway Traffic Safety Administration, http://www.safercar.gov/Rollover

[14] S.M. Shariamadar, M. Manteghi, and M. Tajdari, Enhancement of Articulated Heavy Vehicle Stability by Optimal Linear Quadratic Regulator (LQR) Controller of Roll-yaw Dynamics, *International Journal of Automotive Engineering*, Vol.2, No. 2, 2012.

[15] O. Mokhiamar and M. Abe, Examination of different models following types of yaw moment control strategy for improving handling safety of a car-caravan combination, *Proceeding of the IMechE Part D: Journal of Automobile Engineering*, Vol. 217, pp. 561-571, 2008.

[16] Y. He, H. ElMaraghy, and W. ElMaraghy, A design analysis approach for improving the stability of dynamic system with application to the design of car-trailer systems, *Journal of Vibration and Control*, 11(12): 1487-1509, 2005.

[17] W. Deng and X. Kang, Parametric study on vehicle–trailer dynamics for stability control. *SAE Technical Paper*, Paper No: 2003-01-1321, 2003.

[18] R. J. Anderson and E. F. Kurtz, Handling characteristics simulations of car–trailer systems, *SAE Technical Paper*, Paper No: 800545, 1980.

[19] J. R. Ellis, *Vehicle dynamics*, Business Books Limited, London, 1969.

[20] H. B. Pacejka, *Tire and Vehicle Dynamics, Society of Automotive Engineers and Butterworth-Heinemann*, Oxford, chapters 1, 4, 7, and 8, 2002.

[21] O. Mokhiamar, Stabilization of car-caravan combination using independent steer and drive/or brake forces distribution, *Alexandria Engineering Journal*, 54, pp. 315-324, 2015.

[22] M. Plochl, P. Lugner, and A. Riepl, Improvement of Passenger car-trailer behavior by a trailer based control system, *Vehicle System Dynamics Supplement 28*, pp. 438-450, 1998.

[23] D. Fratila and J. Darling, Simulation of coupled car and caravan handling behaviour, *Vehicle System Dynamics*, 26, pp. 397–429, 1996.

[24] R. S. Sharp and M. A. A. Fernandez, Car-caravan snaking. Part 1: the influence of pintle pin friction, *Proc. Instn Mech. Engrs, Part C: J. Mechanical Engineering Science*, 216, 707–722, 2002.

[25] G. Sustersic, I. Perbil, and M. Ambroz, The Snaking Stability of Passenger Cars with Light Cargo Trailers, *Journal of Mechanical Engineering*, Vol. 60 Issue 9, pp. 539-548, 2014.

[26] M. M. Islam, Parallel Design Optimization of Multi-Trailer Articulated Heavy Vehicles with Active Safety Systems, *PhD Thesis, University of Ontario Institute of Technology*, 2013.

[27] Q. Wang, S. Zhu, and Y. He, "Model Reference Adaptive Control for Active Trailer Steering of Articulated Heavy Vehicles", *SAE Technical Paper*, doi: 10.4271/2015-01-1495, 2015.

[28] J. Kang, G. Burkett Jr., D. Bennett, and S. A. Velinsky, Nonlinear Vehicle Dynamics and Trailer Steering Control of the TowPlow, a Steerable Articulated Snowplowing Vehicle System, *Journal of Dynamic Systems*, Measurement, and Control, Vol. 137, 2015.

[29] F. Sorge, On the sway stability improvement of car-caravan systems by articulated connections, *Vehicle System Dynamics*, 2015.

[30] I. Kageyama and R. Nagai, Stabilization of Passenger Car-Caravan Combination using Four Wheel Steering Control, *Vehicle System Dynamics*, Vol. 24, pp. 313-327, 1995.

[31] K. Rangavajhula and H. S. J. Tsao, Active Trailer Steering Control of an Articulated System With a Tractor and Three Full Trailers for Tractor-Track Following, *Int. J. Heavy Veh. Syst.*, 14(3), pp. 271–293, 2007.

[32] Y. He and Q. Wang, Driver-Hardware/Software-in-the-Loop Real-Time Simulations for the Design of Active Trailer Steering Systems of Multi-Trailer Articulated Heavy Vehicles, *Proceedings of the 12th International Symposium on Advanced Vehicle Control*, September 22-26, Tokyo University of Agriculture and Technology, Tokyo, Japan, 2014.

[33] M. A. A. Fernandez and R. S. Sharp, Caravan Active Braking System-Effective Stabilisation of Snaking of Combination Vehicles, *SAE Technical Paper*, Paper No: 2001-01-3188, 2001.

[34] C. Cheng, Enhancing safety of actively-steered articulated vehicles, *PhD thesis, University of Cambridge*, UK, 2009.

[35] C. R. Carlson and J. C. Gerdes, Optimal rollover prevention with steer by wire and differential braking, *Presented at Proceedings of IMECE*. 2003.

[36] R.C. Lin, D. Cebon, and D. J. Cole, Active Roll Control of Articulated Vehicles, *Vehicle System Dynamics*, 26, pp. 17-43, 1996.

[37] D. J. M. Sampson, Active Roll Control of Articulated Heavy Vehicles, *PhD thesis, University of Cambridge*, 2000.

[38] T. Zhu, C. Zong, H. Zheng, C. Tian, and H. Zheng, Yaw/Roll Stability Modeling and Control of Heavy Tractor-Semi Trailer, *SAE Technical Paper*, Paper No: 2007-01-3574, 2007.

[39] L. Mai, P. Xie, and C. Zong, Research on Algorithm of Stability Control for Tractor Semi-trailer, *Proceeding of the 2009 IEEE, International Conference on Mechatronics and Automation*, 2009.

[40] A. D. Mary, A. T. Mathew, and J. Jacob, A Robust H-infinity Control Approach of Uncertain Tractor Trailer System, *IETE Journal of Research*, Vol. 59, Issue 1, 2013

[41] X. Ding, Y. He, J. Ren, and T. Sun, A comparative Study of Control Algorithms for Active Trailer Steering Systems of Articulated Heavy Vehicles, *American Control Conference*, 2012.

[42] T. Sun, E. Lee, and Y. He, Non-Linear Bifurcation Stability Analysis for Articulated Vehicles with Active Trailer Differential Braking Systems, *SAE Int. J. Mater. Manf. 9(3):2016*, doi:10.4271/2016-01-0433.

[43] D. W. Gu, P. H. Petkov, and M. H. Konstantinov, *Robust control design with MATLAB*, 2nd ed. Springer, London, 2013.

[44] G. Yin, N. Chen, J. Wang, and L. Wu, A study of μ synthesis control for Four-wheel steering system to enhance vehicle lateral stability, *Journal of Dynamics Systems, Measurement, and Control*, 133(1):011002, 2011.

[45] M. Corno, M. Tanelli, I. Boniolo, and S. M. Savaresi, Advanced Yaw Control of Four-wheeled Vehicles via Rear Active Differential Braking, *Joint 48th IEEE Conference on Decision and Control and 28th Chinese Control Conference*, 5176 – 5181, 2009.

[46] W. Yuan and J. Katupitiya, DESIGN OF A μ SYNTHESIS CONTROLLER TO STABILIZE AN UNMANNED HELICOPTER, *28th International Congress of the Aeronautical Sciences*, vol. 4, pp. 3317 – 3325, 2012

[47] S. Skogestad and I. Postlethwaite, *Multivariable Feedback Design: Analysis and Design*, 2nd ed. John Wiley & Sons, Inc., 2001.

[48] Y. He and M. M. Islam, An Automated Design Method for Active Trailer Steering Systems of Articulated Heavy Vehicles, *ASME Journal of Mechanical Design*, Vol. 134/041002, pp. 1-15, 2012.

[49] S. M. Karamihas, T. D. Gillespie, and S. M. Riley, Axle Tramp Contributions to the Dynamic Wheel Loads of a Heavy Truck, *International Symposium on Heavy Vehicle Weights and Dimensions*, 4th, 1995.

[50] J. Darling, D. Tilley, and B. Gao, An Experimental Investigation of Car-Trailer High-speed Stability, *Proc. IMechE, Part D: J. Automotive Engineering*, Vol.223, pp. 471-484, 2009.

[51] K. Zhou and J. C. Doyle, *Essentials of Robust Control*, Prentice Hall, 1999.

[52] I. B. Tijani, R. Akmeliawati, A. Legowo, M. Iwan, and A. G. A. Muthalif, Robust H-infinity controller synthesis using Multi-Objectives Differential Evolution Algorithm (MODE) for Two-mass-spring system, *4th International Conference on Modeling, Simulation and Applied Optimization (ICMSAO)*, 2011.

[53] Office of Regulatory Analysis and Evaluation (National Center for Statistics and Analysis), Final Regulatory Impact Analysis: FMVSS No. 126 – Electronic Stability Control Systems, *National Highway Traffic Safety Administration*, U.S. Department of Transportation, 169 pages, 2007.

[54] K. Koibuchi, M. Yamamoto, Y. Fukada, and S. Inagaki, Vehicle Stability Control in Limit Cornering by Active Brake, *SAE Technical Paper*, doi:10.4271/960487, 1996.

[55] National Highway Traffic Safety Administration, http://www.nhtsa.gov/FARS, 2014 data on all crashes in the United States.

Appendix

Appendix A: The Parameters of the CT system

Description	Symbol	Value
Leading Car total mass	m_c	1521 kg
Leading Car sprung mass	m_{cs}	1306 kg
Trailer total mass	m_t	602 kg
Trailer sprung mass	m_{ts}	466 kg
Yaw moment of inertia of the total mass of the car	I_{z1}	1816 kgm^2
Yaw moment of inertia of the total mass of the trailer	I_{z2}	1764 kgm^2
Roll moment of inertia of the sprung mass of the car	I_{xx1}	846.6 kgm^2
Roll moment of inertia of the sprung mass of the trailer	I_{xx2}	708 kgm^2
Roll-yaw product of inertial of the sprung mass of the car	I_{xz1}	0
Roll- yaw product of inertial of the sprung mass of the trailer	I_{xz2}	0
Longitudinal distance between the CG of the car and front axle of the car	a	0.972 m
Longitudinal distance between the CG of the car and rear axle of the car	b	1.807 m
Longitudinal distance between the CG of the car and hitch	d	3.028 m

Longitudinal distance between the CG of the trailer and hitch	e	$2\ m$
Longitudinal distance between the CG of the trailer and axle of the trailer	f	$0.6\ m$
Height of the CG of car sprung mass above roll axis	h_1	$0.325\ m$
Height of the CG of trailer sprung mass above roll axis	h_2	$0.676\ m$
Vertical distance between car roll center and hitch	z_1	$0.305\ m$
Vertical distance between trailer roll center and hitch	z_2	$0.285\ m$
Gravity Acceleration	g	$9.81\ m/s^2$
Roll damping coefficient of the car suspension	cr_1	5000 Nms/rad
Roll damping coefficient of the trailer suspension	cr_2	7000 Nms/rad
Roll stiffness of the car suspension	kr_1	120000 Nm/rad
Roll stiffness of the trailer suspension	kr_2	210000 Nm/rad
Cornering stiffness of car front tires	c_1	120000 N/rad
Cornering stiffness of car rear tires	c_2	110000 N/rad
Cornering stiffness of trailer tires	c_3	45000 N/rad

Appendix B: System Matrices of Linear 5-DOF Model

In Equation (23), system matrix $\mathbf{A} = -\mathbf{M}^{-1}\mathbf{D}$, input matrix $\mathbf{B} = -\mathbf{M}^{-1}\mathbf{F}$ and control matrix $\mathbf{B_c} = -\mathbf{M}^{-1}\mathbf{F_c}$. The non-zero elements of the matrices are listed below,

$\mathbf{M(1,2)} = d * m_{1s} * h_1 - I_{xz1}$

$\mathbf{M(1,5)} = I_{z1}$

$\mathbf{M(1,7)} = m_1 * d$

$\mathbf{M(2,1)} = -cr_1$

$\mathbf{M(2,2)} = z_1 * m_{1s} * h_1 - I_{x1}$

$\mathbf{M(2,5)} = I_{xz1}$

$\mathbf{M(2,7)} = z_1 * m_1 - m_{1s} * h_1$

$\mathbf{M(3,2)} = m_{1s} * h_1$

$\mathbf{M(3,4)} = m_{2s} * h_2$

$\mathbf{M(3,7)} = m_1$

$\mathbf{M(3,8)} = m_2$

$\mathbf{M(4,4)} = e * m_{2s} * h_2 + I_{xz2}$

$\mathbf{M(4,6)} = -I_{z2}$

$\mathbf{M(4,8)} = m_2 * e$

$$\mathbf{M(5,3)} = -cr_2$$

$$\mathbf{M(5,4)} = z_2 * m_{2s} * h_2 - I_{x2}$$

$$\mathbf{M(5,6)} = I_{xz2}$$

$$\mathbf{M(5,8)} = m_2 * z_2 - m_{2s} * h_2$$

$$\mathbf{M(6,2)} = z_1$$

$$\mathbf{M(6,4)} = -z_2$$

$$\mathbf{M(6,5)} = -d$$

$$\mathbf{M(6,6)} = -e$$

$$\mathbf{M(6,7)} = 1$$

$$\mathbf{M(6,8)} = -1$$

$$\mathbf{M(7,1)} = 1$$

$$\mathbf{M(8,3)} = 1$$

$$\mathbf{D(1,5)} = \frac{a * C_1 * (a+d) - b * C_2 * (d-b)}{U} + d * m_1 * U$$

$$\mathbf{D(1,7)} = \frac{C_1 * (a+d) - C_2 * (b-d)}{U}$$

$$\mathbf{D(2,1)} = kr_1 + m_{1s} * g * h_1$$

$$\mathbf{D(2,5)} = \frac{z_1 * (a * C_1 - b * C_2)}{U} + z_1 * m_1 * U - m_{1s} * h_1 * U$$

$$\mathbf{D(2,7)} = \frac{z_1 * (C_1 + C_2)}{U}$$

$$\mathbf{D(3,5)} = \frac{(a * C_1 - b * C_2)}{U} + m_1 * U$$

$$\mathbf{D(3,6)} = m_2 * U - \frac{f * C_3}{U}$$

$$\mathbf{D(3,7)} = \frac{(C_1 + C_2)}{U}$$

$$\mathbf{D(3,8)} = \frac{C_3}{U}$$

$$\mathbf{D(4,6)} = m_2 * e * U - \frac{C_3 * f * (e + f)}{U}$$

$$\mathbf{D(4,8)} = \frac{C_3 * (e + f)}{U}$$

$$\mathbf{D(5,3)} = m_{2s} * g * h_2 - kr_2$$

$$\mathbf{D(5,6)} = z_2 * m_2 * U - m_{2s} * h_2 * U - \frac{z_2 * f * C_3}{U}$$

$$\mathbf{D(5,8)} = \frac{z_2 * C_3}{U}$$

$$\mathbf{D(6,5)} = U$$

$$\mathbf{D(6,6)} = -U$$

$$\mathbf{D(7,2)} = -1$$

$$\mathbf{D(8,4)} = -1$$

$$\mathbf{F(1,1)} = -C_1 * (a + d)$$

$$\mathbf{F(2,1)} = -z_1 * C_1$$

$$\mathbf{F(3,1)} = -C_1$$

$$\mathbf{F_c(4,1)} = 1$$

Appendix C: The Parameters for μ Synthesis Controller

Description	Symbol	Minimum Value	Nominal Value	Maximum Value
Vehicle Speed	U	40 km/h	60 km/h	110 km/h
Leading Car total mass	m_c	1065 kg (-30%)	1521 kg	1980 kg (+30%)
Trailer total mass	m_t	421 kg (-30%)	602 kg	782 kg (+30%)
Yaw moment of inertia of the total mass of the car	I_{z1}	1271 kgm^2 (-30%)	1816 kgm^2	2360 kgm^2 (+30%)
Yaw moment of inertia of the total mass of the trailer	I_{z2}	1235 kgm^2 (-30%)	1764 kgm^2	2293 kgm^2 (+30%)
Cornering stiffness of car front tires	C_1	84000 N/rad (-30%)	120000 N/rad	156000 N/rad (+30%)
Cornering stiffness of car rear tires	C_2	77000 N/rad (-30%)	110000 N/rad	143000 N/rad (+30%)
Cornering stiffness of trailer tires	C_3	31500 N/rad (-30%)	45000 N/rad	58500 N/rad (+30%)
Longitudinal distance between the CG of the car and front axle of the car	a	-	0.972 m	-

Longitudinal distance between the CG of the car and rear axle of the car	b	-	1.807 m	-
Longitudinal distance between the CG of the car and hitch	d	-	3.028 m	-
Longitudinal distance between the CG of the trailer and hitch	e	-	2 m	-
Longitudinal distance between the CG of the trailer and axle of the trailer	f	-	0.6 m	-